A dedicated inhibitory circuit for gating itch in the spinal cord

Kai-Feng Shen[3,4,14], Rita Bardoni[5,14**], Yuxi Zhou[2,8], Sihan Chen[2,8], Jia-Yan Wu[1], Yali Chen[1], Hui Li[4,7], Juan Liu[4], Yu Sun[4,9], Andrea Bighinati[5], Ben-Long Liu[4,10], Jun Wu[1], Na Wang[4,11], Xiao-Fei Gao[4,12], Joseph Jeffry[4], Xueting Liu[4,6], Xian-Yu Liu[4], Zhong-Qiu Zhao[4], Fang Gao[4,13], Yingfu Jiao[8], Ailing Tao[6], Yun-Qing Li[7], Weifeng Yu[8], Zhou-Feng Chen[1,2,4,15*]

[1]Institute of Neurological and Psychiatric Disorders, Shenzhen Bay Laboratory, [2]Shenzhen Medical Academy of Research and Translation, Shenzhen, Guangdong, 518057, China.

[3]Department of Neurosurgery, Xinqiao Hospital, Army Medical University, Chongqing, 400037, China.

[4]Center for the Study of Itch, Washington University School of Medicine, St. Louis, MO 63110, USA.

[5]Department of Biomedical, Metabolic and Neural Sciences (RB) and Department of Life Sciences (AB), University of Modena and Reggio Emilia, Modena, 41125, Italy.

[6]The Second Affiliated Hospital, The State Key Laboratory of Respiratory Disease, Guangdong Provincial Key Laboratory of Allergy & Clinical Immunology, Sino-French Hoffmann Institute, Center for Immunology, Inflammation, & Immune-mediated disease, Guangzhou Medical University, Guangzhou, Guangdong, 510260, China.

[7]Department of Anatomy & K. K. Leung Brain Research Center, The Fourth Military Medical University, Xi'an, Shanxi, 710032, China.

[8]Department of Anesthesiology, Renji Hospital, Shanghai Jiao Tong University School of Medicine; Key Laboratory of Anesthesiology, Shanghai Jiao Tong University, Shanghai, 200001, China.

[9]Department of Anesthesiology, Shanghai Ninth People's Hospital, Shanghai Jiao Tong University School of Medicine, Shanghai, 200011, China.

Present address:

[10]State Key Laboratory of Medical Neurobiology and MOE Frontiers Center for Brain Science, Institutes of Brain Science, Fudan University, Shanghai 200032, China.

[11]Dermatology Hospital of Shandong First Medical University; Shandong Provincial Institute of Dermatology and Venereology, Shandong Academy of Medical Sciences, Jinan, Shandong, 250021, China.

[12]Translational Research Institute of Brain and Brain-Like Intelligence, Department of Anesthesiology, Shanghai Fourth People's Hospital, Tongji University, Shanghai, 200434, China.

[13]Department of Dermatology, The Mark Lebwohl Center for Neuroinflammation and Sensation, Icahn School of Medicine at Mount Sinai, New York, NY 10019, USA.

[14] These authors contributed equally

[15] Lead contact

*Correspondence: chenz@szbl.ac.cn, **Correspondence: rita.bardoni@unimore.it

SUMMARY

Various populations of spinal inhibitory neurons have been implicated in itch inhibition, but the precise mechanisms underlying tonic gating of itch and its inhibition by pain remain incompletely understood. Here, we identify a subset of inhibitory interneurons that uniquely express neurokinin receptor 3 (NK3R) in the spinal cord of mice. NK3R neurons receive monosynaptic input from *Tac1*$^{+}$ sensory neurons, which release substance P (SP) and project directly to gastrin-releasing peptide receptor (GRPR)-expressing neurons that are dedicated to itch transmission. Silencing of NK3R inhibitory neurons disinhibits GRPR neurons and induces neuropathic itch, whereas their activation profoundly impairs itch but not pain transmission. These findings suggest that spinal NK3R inhibitory neurons serve as a pivotal and specific microcircuit for tonically gating of itch, and that the SP-NK3R-GRPR pathway may underlie the inhibition of itch by pain that activates the primary afferents to release SP onto the spinal cord.

KEYWORDS

Spinal dorsal horn; inhibitory interneurons; itch; GRPR neurons; substance P; NK3R neurons.

INTRODUCTION

Itch information is encoded and transmitted via itch-specific neuropeptides released from primary afferents to itch-specific circuits in the spinal cord[1]. Notably, spinal excitatory interneurons expressing gastrin-releasing peptide receptors (GRPR) act as a central convergence point for transmitting distinct types of itch to the brain [1-7]. As a warning signal, itch also evokes an urge to scratch, resulting in rapid and transient suppression of itch sensation. In addition,

brainstem circuits regulate itch and pain in opposing ways [8,9], highlighting the complex mechanisms underlying the antagonism between itch and pain at different levels. Earlier studies indicated that both noxious and innocuous counterstimuli can inhibit itch through inhibiting spinal dorsal horn neurons [10-12]. Accordingly, much of the research on the inhibitory control of itch has focused on identifying spinal inhibitory neurons that act on GRPR neurons. In the spinal cord of mice, several partially overlapping subsets of inhibitory neurons have been examined using distinct mouse Cre lines expressing *neuropeptide Y (Npy)*, *galanin,* and *prodynorphin (Pdyn)* [13-18]. Among them, galanin and NPY neurons have been shown to directly inhibit GRPR neurons via GABA-mediated synaptic inhibition, and all these inhibitory neurons can also inhibit pain [13,15,19-22]. However, developmental ablation of putative inhibitory neurons may also have contributed to dorsal horn circuit adaptation and plasticity and therefore confound interpretation. As a result, whether a dedicated inhibitory circuit that selectively inhibits itch without affecting pain exists in the adult spinal cord remains unresolved. Moreover, the molecular mechanisms that activate these inhibitory circuits remain unknown. Finally, it remains unclear whether an inhibitory circuit tonically gates spontaneous itch but not pain in the adult spinal cord.

G protein-coupled receptors (GPCRs) play a critical role in the transmission of pain and itch [23]. Spinal circuits mediating somatosensory modalities with slow kinetics, such as itch and pleasant touch, can be well defined by the non-overlapping expression of GPCRs activated by neuropeptides released from primary afferents [3,24]. We reasoned that the inhibitory circuit for itch may similarly be defined by GPCR expression, especially those involved in inhibiting itch by counterstimuli with slow kinetics (e.g., chemical pain). For example, intraplantar injection of AITC or mustard oil, a TRPA1 agonist that could induce chemical pain via the activation of TRPA1 nociceptors [25], inhibits itch [8]. Such a pain-mediated itch is through the inhibition of GRPR

neurons via GABAergic transmission within the dorsal horn [26]. This prompted us to search for GPCR-defined inhibitory circuits that can be activated by painful stimuli. Substance P (SP), a well-established neuropeptide involved in various types of pain signaling in sensory neurons [27], belongs to the neurokinin (or tachykinin) family, also comprising neurokinin A (NKA) and neurokinin B (NKB) [28]. All three peptides bind to neurokinin receptors NK1-3 with varying affinity [29]. Numerous studies have shown that a wide array of noxious stimuli, including mechanical, intense noxious thermal, and cold [30,31], electrical, inflammatory, and neuropathic pain [32,33] (for review, see [27,29,34]), can trigger SP release in the spinal cord. This suggests that SP may activate spinal inhibitory neurons expressing NK receptors to suppress itch. In a search for neurokinin receptors expressed in spinal interneurons, we identified NK3R as a GPCR uniquely expressed in a subset of inhibitory neurons within the superficial dorsal horn. In contrast to extensive research on NK1R-expressing projection neurons in pain transmission, which are widely considered to be activated by SP released from primary afferents, NK3R inhibitory interneurons have drawn scant attention. In this study, we tested the hypothesis that NK3R-inhibitory neurons mediate SP-induced inhibition of itch.

RESULTS

NK3R neurons represent a unique population of interneurons in the spinal cord

To examine the anatomical position of NK3R neurons in the spinal cord, we utilized and validated GENSAT's transgenic *Nk3r*-eGFP or *Nk3r*^{GFP} mouse line by *in situ* hybridization (ISH) followed by immunohistochemical staining (IHC) of eGFP. The majority of eGFP cells (91.5%) express *Nk3r*, whereas eGFP captures 72.1% of *Nk3r* neurons (Figure 1A). eGFP was predominantly

localized in outer lamina II (lamina IIo) and a few in lamina I, where CGRP fibers are present (Figure 1B). Some eGFP was co-stained with isolectin B4 (IB4), a non-peptidergic marker in inner lamina II (lamina IIi) (Figure 1C). However, most of the eGFP signals were located dorsal to PKCγ, a marker ventral to IB4 (Figure 1D). Double ISH using RNAscope revealed that approximately 50% of *Nk3r* neurons express the GABAergic marker *Vgat* and *galanin*, which are expressed in inhibitory neurons that gate itch (Figures 1E, 1F, 1I, 1J, and 1O). By contrast, only a smaller fraction of *Nk3r* cells expresses *Npy* (15.5%) and *Pdyn* (20%), respectively (Figures 1G, 1H, 1K, 1L, and 1O). Approximately 45% of *Nk3r* neurons express *Vglut2*, an excitatory neuronal marker (Figures 1M and 1O). However, eGFP does not overlap with NK1R, a marker for lamina I projecting neurons (Figures 1N and 1O). These results indicate that NK3R neurons comprise an approximately equal proportion of excitatory and inhibitory neuronal populations in lamina II of the mouse spinal cord.

Characterization of the electrophysiological properties and afferent inputs of NK3R neurons

We characterized the electrophysiological profiles of NK3R neurons by patch-clamp recordings of NK3R-eGFP neurons. NK3R neurons displayed distinct firing patterns, as evidenced by applying a step-current stimulation at hyperpolarized potentials (Figures 2A-2E; n = 132). The prevalent pattern observed was delayed firing (58.3%), followed by tonic (29.6%), phasic (9.1%), and gap (3.0%) (Figure 2F). Based on previous studies [35,36], cells exhibiting a tonic firing pattern at hyperpolarized potentials (around -80 mV) are primarily inhibitory interneurons, while delayed-firing neurons are predominantly excitatory [37]. We confirmed this observation using VGAT-ChR2-eYFP mice, identifying VGAT-expressing inhibitory interneurons by a channelrhodopsin-2-mediated light-evoked current. We determined NK3R expression by measuring responses to the agonist senktide in the presence of tetrodotoxin, holding neurons at -60 mV (Figures S1A–S1J).

Comparing the proportions of tonic firing neurons between senktide-responsive VGAT+ and VGAT- populations revealed a statistically significant difference: tonic firing occurred in 80% of VGAT+ neurons (8 of 10), but only 8.3% of VGAT- neurons (1 of 12; two-tailed Fisher's exact test, $p = 0.0015$). These findings indicate a strong association between the tonic firing phenotype and senktide-responsive inhibitory interneurons.

We then assessed both passive and active electrophysiological properties in all recorded NK3R neurons from NK3R-eGFP mice that displayed distinct firing patterns (Table S1). Notably, tonic- and delayed-firing neurons exhibited significant differences across several parameters, including latency to the firing of the first action potential, rheobase, action potential threshold, amplitude, and the number of action potentials elicited by depolarizing current injections. These distinctions align with prior findings indicating that excitatory interneurons in the dorsal horn laminae I-II are less excitable and typically require stronger excitatory input for activation than dorsal horn inhibitory neurons [38,39]. Consistently, tonic-firing neurons displayed spontaneous action potential firing at membrane potentials near the resting potential (-55/-60 mV), with a higher frequency than delayed and phasic neurons (Figures S1K and S1L). Hierarchical cluster analysis of all recorded NK3R neurons, based on their electrophysiological profiles, revealed three main clusters. Two of these clusters (C1 and C2, Figure S1M) consisted predominantly of delayed-firing neurons and are likely to represent the majority of excitatory NK3R interneurons. The third cluster (C3) comprised mostly tonic-firing neurons, consisting predominantly of a relatively homogeneous population of inhibitory NK3R interneurons.

Next, to identify the afferent input type of NK3R-eGFP neurons, we applied electrical stimulation to the dorsal root in spinal cord slices with attached roots (Figures 2G-2K). Glutamatergic excitatory postsynaptic currents (EPSCs) were recorded in 48 out of 55 tested neurons. The

absence of evoked EPSCs in the remaining 7 neurons was likely due to the loss of afferent connections during tissue slicing. Among the responsive neurons, 35.5% exhibited EPSCs mediated by both Aδ and C fibers, while 14.6% and 29.2% responded to Aδ or C fiber stimulation alone, respectively. Additionally, 18.7% of neurons received convergent inputs from Aβ fibers in combination with either Aδ or C fibers, and only 2% received purely monosynaptic input from Aβ fibers (Figure 2L). Analysis of the total synaptic inputs to NK3R-eGFP neurons (n = 74) revealed that Aβ fiber inputs were slightly more likely to be monosynaptic (-M) than polysynaptic (-P), Aδ fiber inputs were roughly equally divided between monosynaptic and polysynaptic connections, and the majority of C inputs were polysynaptic (32.4% versus 14.8% monosynaptic) (Figure 2M). Furthermore, analysis of the relationship between synaptic input types and firing patterns showed that high-threshold inputs (Aδ and C fibers) were present across all neuronal subtypes, while low-threshold inputs (Aβ) were prevalent in tonic- and phasic-firing neurons (Figure 2N, n = 43). Taken together, these results demonstrate that NK3R neurons in laminae I and II comprise both excitatory and inhibitory populations and integrate mono- and polysynaptic inputs primarily from Aδ and C primary afferent fibers.

Analysis of the first EPSC evoked by repetitive dorsal root stimulation revealed mean peak amplitudes of 243.6 ±72.3 pA (n=5), 143.8 ±22.2 pA (n=14), and 124.6 ±28.8 pA (n=11) for monosynaptic Aβ, Aδ, and C fibers, respectively. Given that the rheobase for NK3R neurons ranged between 30 and 65 pA when holding the membrane potential around -80 mV (see Table S1), these evoked synaptic currents are in general more than sufficient to trigger action potentials from the resting membrane potential. Accordingly, recordings of EPSPs evoked by dorsal root stimulation exhibited superimposed action potentials in 5 out of 6 tested NK3R neurons (Fig. 2O).

NK3R neurons respond to capsaicin and menthol

We previously reported that inflammatory pain-induced chemical stimuli and cooling can inhibit GRPR neurons [26]. This prompted us to assess whether NK3R neurons receive afferent inputs expressing TRPV1 or TRPM8 receptors. We tested the effects of capsaicin and menthol on glutamatergic spontaneous EPSCs (sEPSCs) recorded in voltage clamp at -70 mV. Bath application of 1 μM capsaicin evoked a significant increase in sEPSC frequency in 13 out of 14 NK3R neurons (Figures 2P and 2Q), and the enhancement persisted in the presence of tetrodotoxin (TTX, 1 μM) in a separate sample of NK3R neurons (Figure 2R, 13/13 of recorded neurons), showing that NK3R neurons receive monosynaptic inputs from TRPV1-expressing terminals. Effects of capsaicin on the amplitude of sEPSCs and miniature EPSCs (mEPSCs) were not determined since, at this capsaicin concentration, the currents are often summated, and the amplitude measure is not accurate. Combining the analysis of firing patterns characterized during initial recordings, capsaicin-responsive NK3R neurons encompassed all physiological firing types (Figure 2S).

A subpopulation of NK3R neurons responded to 500 μM menthol with a significant increase in sEPSCs (5 of 7 recorded neurons; Figures 2T and 2U). In a separate sample of NK3R neurons, menthol significantly increased mEPSC frequency in the presence of TTX (9/20 neurons, Figure 2V), while mean mEPSC amplitude remained unchanged in the responsive neurons, suggesting a presynaptic effect (Figure 2W). These findings indicate that NK3R neurons receive inputs from TRPM8 terminals. In contrast to capsaicin, menthol application enhanced mEPSC frequency primarily in tonic-firing (responsive: 5/7) and phasic-firing (responsive: 2/3) NK3R neurons, with lower responsiveness detected in delayed-firing neurons (responsive: 2/10) (Figure 2X). These

results demonstrate that NK3R neurons, particularly the inhibitory ones, integrate inputs from TRPM8-expressing afferent fibers.

Ablation or inhibition of NK3R inhibitory neurons results in neuropathic itch

To determine the functional role of NK3R neurons, we next employed a toxin-based chemical ablation approach and performed intrathecal injections (i.t.) of NKB-saporin (NKB-sap) in the lumbar section of C57BL/6J mice. Surprisingly, 3 ~ 4 days after i.t. NKB-sap, about 90% of mice began to develop robust spontaneous scratching/biting behavior, followed by skin lesions one week later (Figures 3A and 3C, and S2A). Moreover, scratching behavior elicited by intrathecal (i.t.) GRP, and neuromedin B (NMB, a neuropeptide that encodes histamine itch [7,40]) was significantly enhanced in NKB–sap-treated mice (Figures S3A and S3B). In contrast, intradermal injection (i.d.) of chloroquine (CQ, a nonhistaminergic pruritogen mediated in part by GRP-GRPR signaling[2]) and histamine-induced scratching, along with mechanical itch, showed no significant changes (Figures S3C–S3E). To test whether these behaviors may be an indicator of spontaneous pain, we injected morphine intraperitoneally (i.p.), which failed to suppress scratching/biting behavior (Figures 3B and S2B). To further test whether spontaneous scratching/biting behavior may reflect neuropathic itch, we conducted i.t. injection of bombesin (BB-sap), which abolishes itch by ablating GRPR neurons [3], followed by i.t. NKB-sap (Figure 3D). Notably, these mice failed to exhibit spontaneous scratching/biting behaviors (Figures 3E and S2C), suggesting that the robust scratching/biting behaviors observed in mice treated with NKB-sap are primarily driven by spontaneous itch rather than pain.

ISH studies confirmed that a majority of *Nk3r* cells were ablated in the dorsal horn of mice treated with NKB-sap (Figures 3F and 3G). In contrast, NK1R expression was comparable between mice

treated with saline and NKB-sap, demonstrating NKB-sap specificity (Figures 3H and 3I). Expression of GABA was also reduced substantially in mice treated with NKB-sap (Figures 3J and 3K). Importantly, GRPR expression was significantly enhanced in the dorsal horn of mice treated with NKB-sap (Figures 3L and 3M), indicating that heightened spontaneous scratching/biting behaviors occur as a result of disinhibition of GRPR neurons. Additionally, the expression of GABAergic Pax2 neurons was significantly reduced in the dorsal horn of mice treated with NKB-sap (Figures S2D and S2E). The expression of c-Fos-positive neurons was increased in the superficial dorsal horn (Supplementary Figures S2F and S2G) and co-expressed in GRPR neurons (Figures S2H and S2I), but barely in GABA neurons (Figures S2J and S2K).

To further assess the role of NK3R inhibitory neurons, we generated *Nk3r-Cre* or *Nk3r*^{iCre} mice using a gene targeting strategy and confirmed that *iCre* and *Nk3r* expression largely overlap in the spinal cord. 97.7% of *Nk3r* cells expressed *iCre*, whereas *iCre* captured approximately 93.4% of *Nk3r* neurons (Figures 4A and 4B). We then injected AAV2/8-Vgat-DIO-h4MDi-mCherry into the cervical spinal cord of Nk3riCre mice, allowing selective inhibition of NK3R inhibitory neurons with i.p. clozapine. ISH staining and quantitative analysis showed that over 85% mCherry-positive neurons co-expressed *Nk3r* and *Vgat* in the infected spinal cord (Figures 4C and 4D). Consistent with ablation studies, clozapine-mediated selective inhibition of NK3R inhibitory neurons resulted in robust spontaneous scratching behavior (Figure 4E).

To verify the result obtained from *Nk3r*^{iCre} mice, we also generated *Nk3r*^{DTR} mice for *Nk3r* ablation (Figure 4F). To ablate spinal cord *Nk3r* neurons, diphtheria toxin (DTX) was injected (i.p.) at day 0, 4, 7, and 14 (Figure 4G). Selective ablation of *Nk3r* neurons resulted in robust spontaneous scratching behavior (Figure 4H), while injection of the GRPR antagonist JMV594 significantly abolished the scratching behavior of *Nk3r*^{DTR} mice injected with DTX (Figure 4I).

The ISH results further confirmed that *Vgat*$^{+}$/*Nk3r*$^{+}$ neurons were decreased in the spinal cord of *Nk3r*^{DTR} mice (Figures 4J and 4K). In conclusion, these findings further establish that ablation of NK3R neurons leads to neuropathic itch, and that this effect is mediated by GRPR neurons.

Activation of NK3R neurons inhibits itch without impacting pain behavior

Next, we examined the effect of activation of NK3R neurons on itch using a pharmacological approach. We first evaluated the dose-dependent effects of NKB (10 pmol, 100 pmol, and 1 nmol) on i.t. GRP-induced pruritus. While the two lower doses did not elicit any notable change in scratching behavior, the 1 nmol dose significantly suppressed scratching (Figure S4), so we used this concentration for subsequent experiments. We found that i.t. administration of NKB significantly inhibited scratching behavior elicited by i.t. GRP, i.d CQ, NMB, and histamine (Figures 5A-5D). NKB also markedly suppressed scratching behavior induced by i.t. morphine, which is mediated by MOR1D/GRPR crosstalk in the spinal cord of mice[41] (Figure 5E). Moreover, NKB significantly inhibited scratching behavior elicited by dry skin, a mouse model of chronic itch that resembles the human dry skin itch condition [42] (Figure 5F). To test NKB specificity for NK3R activation, we evaluated its effect on itch in *Nk3r* knockout (KO) mice. i.t. administration of NKB failed to inhibit scratching behavior elicited by i.t. GRP (Figure 5G), demonstrating that NK3R is essential for the itch-suppressing effect of NKB.

We next examined the effect of i.t. NKB administration on pain behavior. Unexpectedly, we did not detect a significant difference in pain induced by thermal, mechanical, and cold stimuli (Figures S5A-S5E). Pain induced by capsaicin, chemical pain induced by Complete Freund's adjuvant (CFA), and neuropathic pain generated by spared nerve injury (SNI), were also not

affected by i.t. NKB (Figures S5F-S5I). These results indicate that exogenous NKB does not affect nociceptive transmission.

Finally, we employed a chemogenetic approach to selectively activate NK3R inhibitory neurons by expressing AAV2/8-Vgat-DIO-hM3Dq-mCherry virus in the cervical spinal cord in *Nk3r*^{iCre} mice. c-Fos staining confirmed the activation of mCherry-positive neurons by clozapine injection (Figure 5H). Consistently, chemogenetic activation of NK3R inhibitory neurons with DREADD (i.p. clozapine) profoundly impaired scratching behaviors induced by i.t. GRP, CQ, histamine, and dry skin (Figures 5I-5L). These findings further demonstrate that activation of NK3R inhibitory neurons does not affect nociceptive transmission (Figure S6).

NK3R neurons form monosynaptic contacts with Tac1 sensory neurons

To explore whether *Tac1*-expressing primary afferents form monosynaptic contacts with NK3R neurons, we carried out rabies virus–mediated retrograde tracing by injecting glycoprotein (G)–deleted rabies virus (RVdG) in the spinal cord of *Nk3r*^{iCre} mice (Figures 6A and 6B), as we previously described [24]. Examination of *Tac1* expression with retrograde transported RVdG that labels the input neurons with DsRed in DRGs revealed that approximately 41% of input neurons were colocalized with *Tac1* (Figure 6C). DsRed and *Tac1* co-expression was also found in the spinal cord (Figure 6D). These results demonstrate that SP-expressing neurons form monosynaptic contacts with NK3R neurons, consistent with the central innervation of SP fibers in spinal cord lamina II.

To confirm the expression of functional NK3Rs on NK3R-eGFP neurons, we applied 1 μM NKB while recording in voltage clamp at -60 mV (Figure 6E). We found that 12 out of 20 neurons were responsive to NKB, exhibiting a slow inward current (mean amplitude: 11.5 ± 1.3 pA)

(Figures 6F and 6I). To confirm that this slow response resulted from activation of NK3R receptors on the recorded neurons, we applied the more selective NK3R agonist senktide (1 μM) in the presence of TTX. Under these conditions, similar inward currents were observed in 17 of 23 NK3R neurons (mean amplitude: 19.4 ± 2.6 pA; Figures 6G and 6I), confirming that they result from the direct activation of NK3R on the recorded neurons. Both tonic- and delayed-firing NK3R neurons responded to senktide, confirming that functional NK3Rs are expressed on both inhibitory and excitatory interneurons (Figure 6J). Finally, a subpopulation of NK3R neurons (26 out of 37) exhibited an inward current in response to 2 μM SP, which represents the principal endogenous agonist for NK3R in the dorsal horn (mean amplitude of SP-induced current: 6.5 ± 0.7 pA; Figures 6H and 6I). Application of SP in the presence of the NK3R antagonist SB 223412 (3 μM) did not evoke any response, confirming that the SP-mediated effects were due to NK3R activation (Figure 6K).

NK3R neurons inhibit GRPR neurons via GABAergic transmission

Finally, we took advantage of the finding that NK3R and GRPR are expressed in distinct populations of interneurons (Figure 7A) and examined whether the former forms monosynaptic contacts with the latter (Figure 7B) in *Grpr*^{iCre} mice, using the rabies virus circuit tracing method as we previously described[5]. With glycoprotein in the starter neurons (yellow), retrogradely transported RVdG would track the input neurons expressing dsRed (Figure 7C). RNAscope studies revealed that most *Nk3r* neurons that overlap with DsRed also express *Vgat* (Figure 7C), demonstrating that NK3R inhibitory neurons form monosynaptic connections with GRPR neurons.

To further investigate the hypothesis that inhibitory NK3R neurons form direct synaptic contacts with GRPR neurons, we performed voltage clamp experiments at -10 mV on GRPR-eGFP

neurons and tested the effect of NKB on sIPSCs and mIPSCs (Figure 7D). NKB (1μM) caused a significant increase in sIPSC frequency in 11/31 GRPR neurons (Figures 7E and 7F), without affecting sIPSC amplitude (Figure 7G). The application of bicuculline (20 μM) at the end of the experiment blocked most of the sIPSCs, showing that they were mediated mainly by $GABA_A$ receptors (Figures 7E and 7H). After the addition of 500 nM strychnine, the residual sIPSCs were blocked entirely in all neurons. Application of NKB did not significantly alter the frequency of spontaneous glutamatergic EPSCs (sEPSCs) in the subset of GRPR neurons where these events were clearly detectable as inward currents (Figure 7I), suggesting that activation of excitatory NK3R neurons by NKB does not influence GRPR neuron activity.

The effect of NKB on sIPSCs recorded from GRPR neurons was prevented by the application of the NK3R antagonist SB223412 (3 μM), as only one out of 17 neurons showed a significant increase in sIPSC frequency in the presence of NKB and SB223412 (Figures 7J and 7K). This result confirms that NKB selectively activates NK3Rs on inhibitory NK3R-expressing neurons, increasing GABA (and glycine) release. Co-application of NKB with TTX did not abolish the effect of NKB on mIPSCs, as 7 of 21 GRPR neurons still exhibited a significant increase in mIPSC frequency (Figures 7L and 7M). NKB did not significantly alter the mean amplitude of mIPSCs recorded from responsive GRPR neurons (Figure 7N), indicating a modulatory effect of NKB at the presynaptic terminals of NK3R neurons and confirming that GRPR neurons receive monosynaptic inputs from inhibitory NK3R neurons.

DISCUSSION

In this study, we identify a distinct population of NK3R interneurons innervated by *Tac1* primary afferents in mice. We show that capsaicin, menthol, and neurokinins can activate NK3R neurons,

which inhibit GRPR neurons through monosynaptic GABAergic transmission. Our data suggest that the SP-NK3R-GRPR molecular and neural pathways underlie pain-mediated inhibition of itch. The observation that ablation of NK3R neurons induces robust spontaneous scratching, while their activation inhibits itch—without affecting pain-related behavior—highlights the specificity of NK3R inhibitory neurons in regulating itch. NK3R neurons appear to inhibit itch through two distinct mechanisms: (a) they exert tonic suppression of GRPR neurons, independent of SP; (b) they mediate peripheral input-dependent itch inhibition, which may or may not engage SP, depending on the nature of counterstimuli. Together, NK3R inhibitory neurons represent a functionally specialized microcircuit that selectively inhibits itch, but not pain. These findings fill a critical gap in our understanding of how counterstimuli inhibit itch.

Our study provides an extensive characterization of the passive and active membrane properties of NK3R neurons, together with their primary afferent-mediated synaptic inputs and responsiveness to counterstimuli (Tables S1 and S2). The analysis of the various electrophysiological profiles in NK3R neurons revealed notable differences in neuronal excitability, especially between tonic-firing (putative inhibitory) and delayed-firing (putative excitatory) types (Table S1 and Figure S1). Consistent with previous studies [36,38,43], tonic-firing NK3R neurons exhibit higher excitability, evidenced by their lower rheobase, lower action potential threshold, shorter latency to the first spike (Table S1), and their ability to fire action potentials spontaneously (Figure S1). Given these properties, tonic-firing NK3R neurons may be activated by low levels of excitatory neurotransmitters and/or exhibit spontaneous activity[44], resulting in prolonged inhibition of postsynaptic neurons.

Previous characterization of dorsal horn inhibitory interneurons for itch mainly focused on peptidergic neurons [13-15,45]. However, these neurons are also implicated in pain, and some

neuropeptides are expressed in excitatory neurons [15,19-21]. NK3R inhibitory neurons functionally are reminiscent of galanin neurons, as both inhibit GRPR neurons via GABAergic transmission, and most, if not all, NK3R inhibitory neurons co-express *galanin* (Table S2). NK3R inhibitory neurons also share similarities with PrP-eGFP neurons, which comprise approximately 60% galanin neurons, exhibit a predominant tonic firing pattern, and form direct connections with TRPV1 and TRPM8 fibers [46]. By contrast, NK3R inhibitory neurons seem to differ from *Npy* neurons, which exhibit low sensitivity to capsaicin, a lack of response to the TRPM8 agonist icilin, and a higher input resistance [47], even though they share a predominant tonic firing pattern, similar resting potentials and action potential amplitudes, along with the capacity to release GABA onto GRPR neurons [15,43]. This would suggest that a small minority of NK3R neurons, which are insensitive to menthol and smaller in size (correlated with higher input resistance), may express NPY.

Intriguingly, ablation of galanin neurons does not give rise to spontaneous itch [13], in contrast to NPY neurons [15], which may also disinhibit pain circuits. Removing NK3R-negative galanin neurons—which comprise a majority of the galanin population—may offset the effects of ablating NK3R inhibitory neurons. In contrast, the neuropathic itch arising from NK3R neuron ablation resembles that observed with the loss of Ptf1a^{Cre}-lineage neurons [43], supporting the notion that NK3R inhibitory neurons may be derived from Ptf1aCre-lineage neurons.

Coupled with a large amount of evidence indicating that SP is released from primary afferents in response to noxious stimuli [48], it is reasonable to assume that SP and glutamate are co-released from primary afferents onto the dorsal horn to activate NK3R neurons, thereby inhibiting itch. The finding that NK3R inhibitory neurons could also be activated by innocuous scratching behavior indicates their broader role in itch regulation. Moreover, it suggests that NK3R inhibitory neurons

can be activated in a SP-independent manner. Since nearly one-third of the afferent fibers synapsing onto tonic-firing NK3R neurons are low-threshold Aβ fibers, scratching may likely activate innocuous mechanoreceptor afferents, leading to glutamate release to activate NK3R neurons directly. It is also possible that scratching may activate laminae III–IV interneurons, which then excite NK3R neurons [49,50].

Because glutamate mediates the transmission across multiple somatosensory modalities, both from primary afferents to the dorsal horn and between different subsets of excitatory dorsal horn neurons [5,51,52], its release from various subsets of primary afferents must be precisely regulated by hardwired pathways in a temporally controlled manner to ensure high-fidelity transmission or inhibition of itch. We and others have shown that GABA is necessary and sufficient to mediate the rapid inhibition of GRPR neurons [13,15,26]. This raises the question of the role of endogenous inhibitory neuropeptides in inhibiting itch, given that several of them partially overlap with NK3R inhibitory neurons. A careful examination of the literature, however, fails to yield convincing loss-of-function evidence demonstrating the role of a spinal inhibitory neuropeptide in itch inhibition. In fact, most studies employed exogenous administration of inhibitory neuropeptides to activate endogenous receptors to infer their endogenous function in itch [5,17,18,20,53,54]. However, such exogenously induced activation could be an artifact, as the relatively high dose of neuropeptides used does not mimic their endogenous release or function. For instance, we have shown that i.t. DYN activates kappa opioid receptors on GRPR neurons, triggering a noncanonical signaling cascade that leads to GRPR phosphorylation, a process not typically engaged under physiological conditions, but a loss of either *Dyn* or *Dyn* neurons has no impact on itch [19,54]. Similarly, i.t. NPY can inhibit itch via NPY1R on GRPR neurons [5], or inhibit pain by targeting NPY1R on spinal nociceptive neurons [15,20,55]. Despite a large body of studies, evidence for spinal-restricted knockout

of NPY remains lacking. Although ablation or inhibition of these inhibitory neuron subsets may disinhibit itch, this effect can be fully accounted for with GABAergic inhibition. Consistent with this notion, mice lacking *Tac2*, *Pdyn*, and *Grp* in the spinal cord exhibited normal itch behaviors [5,19,56,57], demonstrating that these locally-derived neuropeptides are dispensable for itch.

NKB is an endogenous ligand for NK3R, but it is selectively expressed in the dorsal spinal cord rather than in sensory neurons [5,29,56]. While *Tac2* neurons in the spinal cord are essential for mechanical itch, NKB does not appear to play a role in itch or pain [5,56], leaving the endogenous ligand in sensory neurons for NK3R unsolved. The present findings suggest that SP in primary afferents acts as an endogenous ligand for NK3R, despite NK3R exhibiting higher binding affinity for NKB and NKA than SP [58,59]. This may help resolve a long-standing discrepancy: while SP-containing fibers densely innervate laminae I-IIo, overlapping with GRP/TRPV1/CGRP fibers [57,60], NK1R neurons are confined to lamina I. Traditionally, NK1R has been considered the sole receptor for SP in the superficial dorsal horn [33,61-63]. Our results call for a reassessment of the roles of SP and its receptors (NKRs) in somatosensory transmission. Although i.t. NKB did not alter pain behaviors, the potential involvement of excitatory NK3R-expressing neurons in nociceptive processing remains an open question and warrants further investigation.

Neuropathic itch, caused by injury to the nervous system, is a significant clinical challenge with poorly understood mechanisms [64,65]. Ectopic activation of GRP-expressing sensory neurons may amplify GRPR signaling, probably by recruiting neurons expressing *Grpr* mRNA, a process called cross-sensitization under pathological conditions, in the spinal cord, leading to spontaneous itch and skin lesions that resemble neuropathic itch [66]. Alternatively, direct disinhibition of GRPR neurons by a loss or downregulation of NK3R inhibitory neurons could also contribute to this condition. Of a number of inhibitory neurons for itch examined, NK3R inhibitory neurons remain

the only ones whose ablation or inhibition in the adult spinal cord results in spontaneous neuropathic itch. This work supports a hardwired inhibitory neuronal circuit dedicated to itch, embedded within a mix of excitatory neurons from different somatosensory modalities in the dorsal horn. Importantly, ligand-based pharmacological and genetic approaches can selectively activate or inhibit NK3R neurons, making them highly accessible for functional and electrophysiological analysis. This presents a unique opportunity to investigate their role under various physiological and pathological states. Dysregulation of NK3R neuron–mediated inhibitory control may underlie or exacerbate chronic itch conditions that are often resistant to current therapies.

Limitations of the study

Several limitations of the present study warrant acknowledgment. First, NK3R neurons comprise both excitatory and inhibitory subtypes, making selective electrophysiological characterization of NK3R inhibitory neurons challenging. To address this, we examined the firing patterns while holding neurons at hyperpolarized potentials – a protocol previously shown to reliably identify inhibitory interneurons as tonic-firing cells [37]. Consistent with this, experiments using the VGAT-ChR2-eYFP mouse model confirmed that the majority of tonic-firing NK3R neurons are inhibitory interneurons. Second, modeling pain-mediated inhibition of itch in behaving mice is not feasible, as nocifensive behaviors would inherently interfere with itch-related scratching. Moreover, conventional inflammatory pain-inducing agents are typically injected into the hindpaw and engage the lumbar spinal cord, whereas itch is routinely assessed at the cervical level. Finally, although our data highlight the essential role of NK3R inhibitory neurons in gating spontaneous

itch, it remains to be elucidated whether distinct NK3R inhibitory neuron subtypes mediate tonic gating versus counterstimuli-evoked inhibition of itch.

RESOURCE AVAILABILITY

Requests for further information and resources should be directed to and will be fulfilled by the lead contact, Zhou-Feng Chen (chenz@szbl.ac.cn).

Materials availability

Materials and reagents will be available upon reasonable request.

Data and code availability

The data reported in this paper are available upon request.

ACKNOWLEDGMENTS

We thank D. Barry, Y. Zhang, Q. Yang, H. Jin, J. Yin, and J. Cen for their contributions to the project and technical support. The project was supported by the R01NS094344 (Z. F. C), the National Natural Science Foundation of China W2431025 (Z. F. C), Guangdong Pearl River Funding (Grant No. 2023ZT10Y018) (Z. F. C), and Shenzhen Bay Laboratory Fund 21290071 (Z. F. C), Special Program for Discipline Talent Cultivation of Xinqiao hospital (2024XKRC007) (K. F. S.), FAR program, University of Modena and Reggio Emilia, and “Fondo di Beneficienza ed opere di carattere sociale e culturale di Intesa Sanpaolo” (project B/2023/0143) (R.B.).

AUTHOR CONTRIBUTIONS

K.F.S. and R.B. designed the experiments, performed tests, analyzed the data, and contributed to the writing of the manuscript. Y. Z. and S. C. performed chemogenetic experiments and analysis. H. L., J. L., Y. C., and Z.Q.Z. contributed to IHC and RNAscope experiments. X.F.G. and J.J. participated in the electrophysiological recording experiment. Y.S., N.W., J. W., and B.L.L. helped with behavioral studies. A.B., X.L., X.Y.L., F.G., Y.J., A.T., Y.Q.L., J.Y.W., and W.Y. contributed to various parts of the project. Z.F.C. conceived and supervised the project. Z.F.C., K.F.S., and R.B. wrote the manuscript.

DECLARATION OF INTERESTS

The authors report no competing interests.

SUPPLEMENTAL INFORMATION

Supplemental Figures S1–S6 and Tables S1 and S2

FIGURE TITLES AND LEGENDS

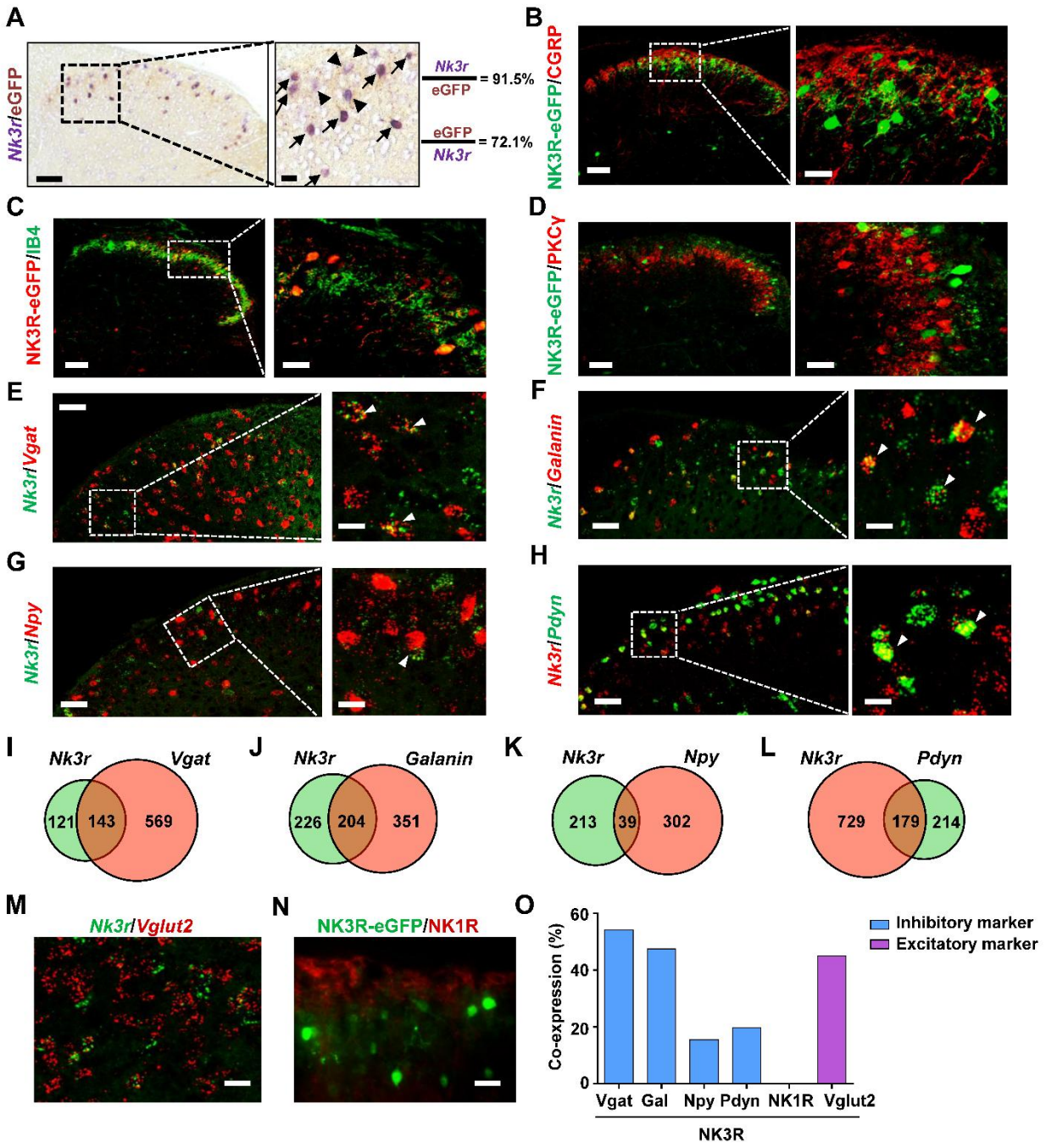

Figure 1. NK3R neurons comprise both inhibitory and excitatory neurons.

(A) ISH images showing co-expression of *Nk3r* and eGFP in the superficial dorsal horn. *Nk3r* mRNA was detected in 91.5% of eGFP neurons, and 72.1% of *Nk3r* neurons express eGFP. Arrowheads indicate *Nk3r*-positive neurons. Arrows indicate *Nk3r*/eGFP double-positive neurons.

(B-D) Double IHC images illustrating the expression pattern of NK3R-eGFP neurons in the superficial dorsal horn relative to CGRP (B), IB4 (C), and PKCγ (D). **(E-L)** Representative images of double FISH using RNAscope probes (E-H) and Venn diagrams (I-L) showing that *Nk3r* neurons express *Vgat* (E and I), *Galanin* (F and J), *Npy* (G and K), and *Pdyn* (H and L). Arrowheads indicate double-positive cells. **(M)** Double ISH image showing that *Nk3r* neurons (green) express *Vglut2* (red). **(N)** IHC image shows that NK3R-eGFP neurons (green) and NK1R (red) do not overlap. **(O)** Percentage of expression of inhibitory and excitatory markers in NK3R neurons. Scale bars: 100 μm (low magnification), 20 μm (high magnification) for (a-l); 20 μm for (m, n). *n* = 3-5 mice for each group.

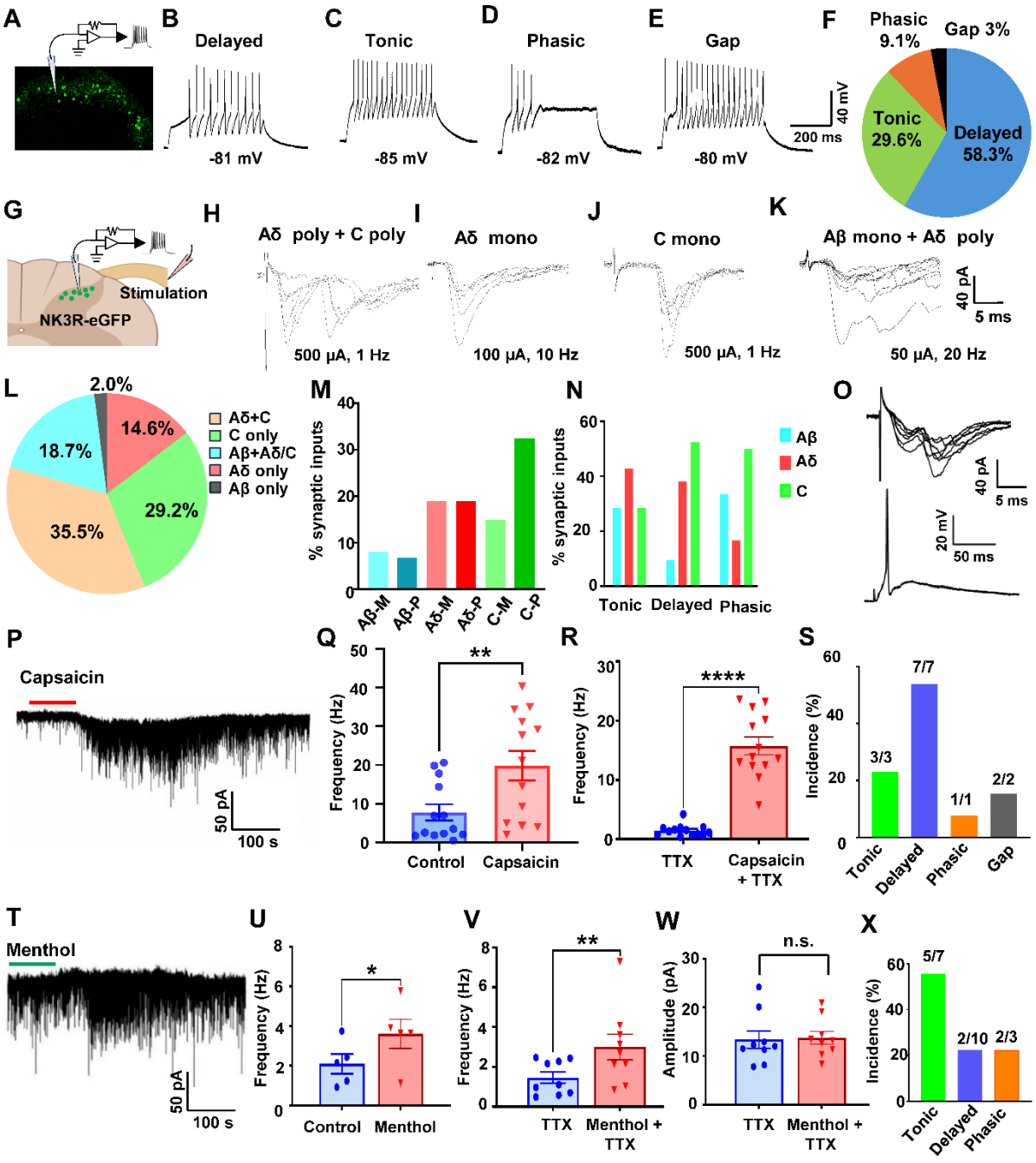

Figure 2. Electrophysiological characterization of NK3R neurons.

(A) Diagram illustrating the recording of an eGFP-positive neuron from a spinal cord slice obtained from an NK3R-eGFP mouse. **(B-E)** Representative delayed, tonic, phasic, and gap firing

patterns recorded from NK3R neurons, each initiated from hyperpolarized membrane potentials (indicated below each panel). **(F)** Pie chart representing the percentages of delayed (58.3%), tonic (29.6%), phasic (9.1%), and gap (3%) firing patterns obtained from a sample of 132 NK3R neurons. **(G)** A diagram showing the recording of NK3R-eGFP neurons in the superficial dorsal horn and stimulation of the dorsal root. **(H-K)** Representative traces of EPSCs recorded from NK3R neurons, evoked by dorsal root stimulation at different intensities. **(L)** Percentages of the different afferent inputs from a sample of 48 NK3R-eGFP neurons. **(M-N)** Percentages of monosynaptic (–M) and polysynaptic (–P) responses among the 74 synaptic inputs examined, along with the distribution of synaptic input types across firing patterns (N). **(O)** Example trace of evoked EPSCs mediated by monosynaptic Aδ and C fibers (top) and the corresponding EPSP (bottom), recorded at the cell resting potential and showing a superimposed action potential. **(P)** Representative trace showing a significant increase of sEPSC frequency elicited by capsaicin. **(Q-R)** sEPSC and mEPSC frequency changes caused, in the responsive neurons, by application of 1 μM capsaicin (Q: $^{**}p < 0.01$, $n = 13/14$) and 1 μM capsaicin + 1 μM TTX (R: $^{****}p < 0.0001$, $n = 13/13$). Responsive neurons were assessed by applying the Kolmogorov-Smirnov test on EPSC inter-event intervals. **(S)** Percentage incidence of the different firing patterns observed in NK3R neurons responsive to capsaicin + TTX. Numbers above the bars indicate the responsive neurons. **(T)** Example of an NK3R neuron where sEPSC frequency was significantly enhanced by application of 500 μM menthol. **(U-V)** sEPSC and mEPSC frequency increases were observed in responsive neurons following application of menthol (U: control 2.1 ± 0.5 Hz, menthol 3.6 ± 0.7 Hz, n = 5/11; paired *t*-test, $^{*}p < 0.05$, n = 5) and menthol + 1 μM TTX (V: control 1.4 ± 0.2 Hz, menthol 3.0 ± 0.6 Hz, n = 9/20; Wilcoxon Signed Rank test, $^{**}p < 0.01$, $n = 9$). **(W)** Amplitudes of mEPSCs were not altered by menthol in the responsive neurons (mean amplitude in TTX: 13.4 ± 1.8 pA, TTX +

menthol: 13.7 ± 1.3 pA, paired t-test, $p = 0.54$, $n = 9$). **(X)** Percentage incidence of the different firing patterns observed in NK3R neurons responsive to menthol + TTX. Numbers above the bars indicate the responsive neurons.

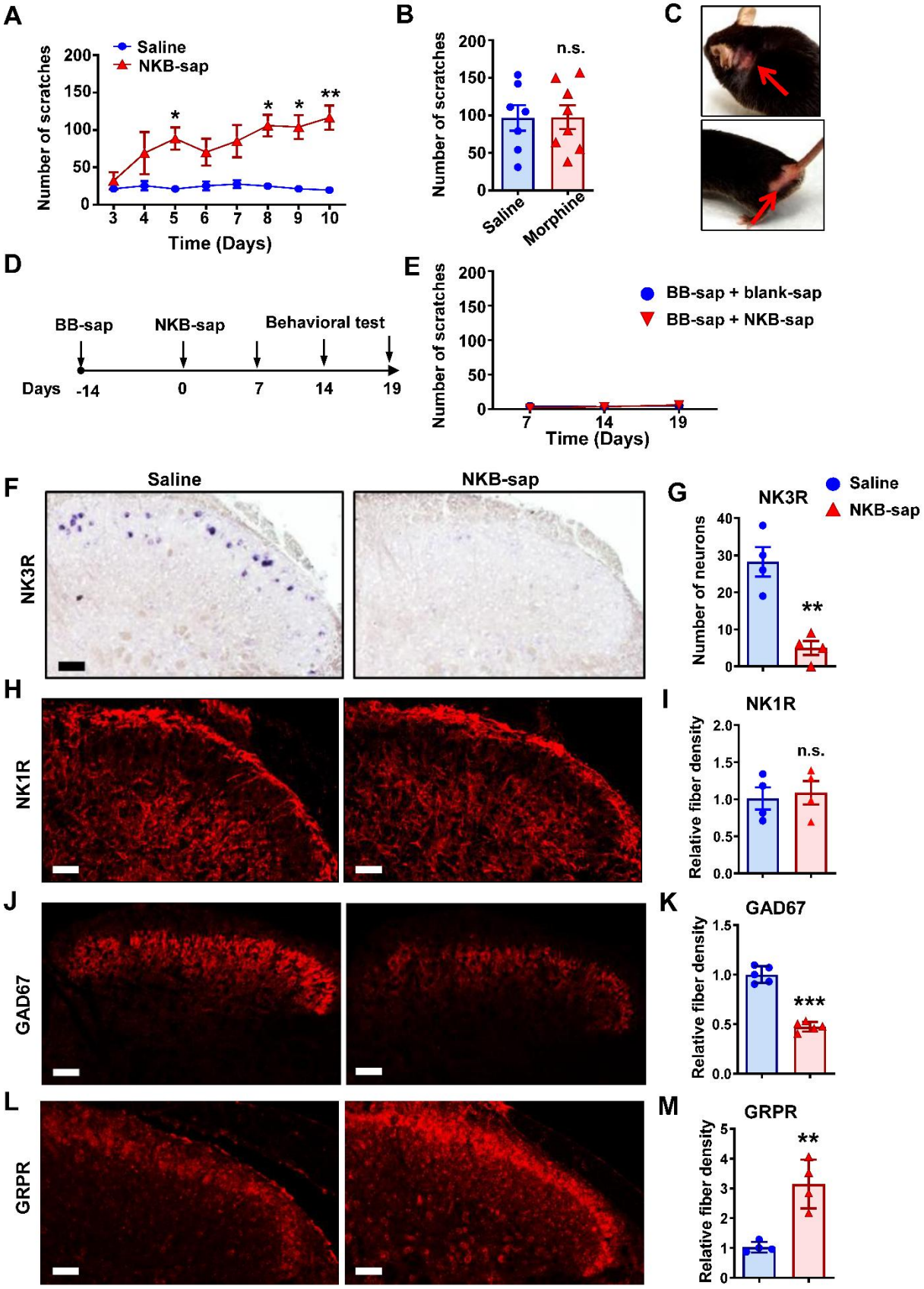

Figure 3. Ablation of NK3R neurons results in neuropathic itch.

(A) NKB-sap treatment caused robust spontaneous scratching behaviors starting at day 5. n = 7-8 mice per group. *$p < 0.05$, **$p < 0.01$, two-way ANOVA with Bonferroni *post-hoc* test. **(B)** Morphine (0.3 nmol, i.t.) did not affect the spontaneous scratching behaviors of NKB-sap-treated mice. n = 7-8 mice per group. n.s., not significant. **(C)** Representative images showing that mice treated with NKB-sap developed skin lesions on the neck and perianal skin due to scratching and biting, respectively. **(D-E)** Schematic timeline of BB-sap and NKB-sap treatment before behavioral tests (D). After ablation of GRPR neurons with BB-sap (500 ng, i.t.), NKB-sap injections did not evoke spontaneous scratching for up to 19 days (E). n = 6-7 mice per group. **(F-G)** ISH images (F) and quantified data (G) representing the ablation of *Nk3r* neurons in the superficial dorsal horn after injection of NKB-sap. Scale bar, 100 μm. n = 4 mice per group. **$p < 0.01$, unpaired t-test. **(H-I)** IHC images (H) and quantified data (I) demonstrating that the expression of NK1R in the spinal cord is not affected by NKB-sap treatment. Scale bars, 100 μm. n = 4 mice per group. n.s., not significant. **(J-M)** IHC images (J-L) and quantified data (K-M) showing that NKB-sap treatment significantly decreases the number of $GABA^+$ cells (J-K), while enhancing the number of $GRPR^+$ cells (L-M) in the dorsal horn. n = 4-5 mice per group. *$p < 0.05$, unpaired t-test.

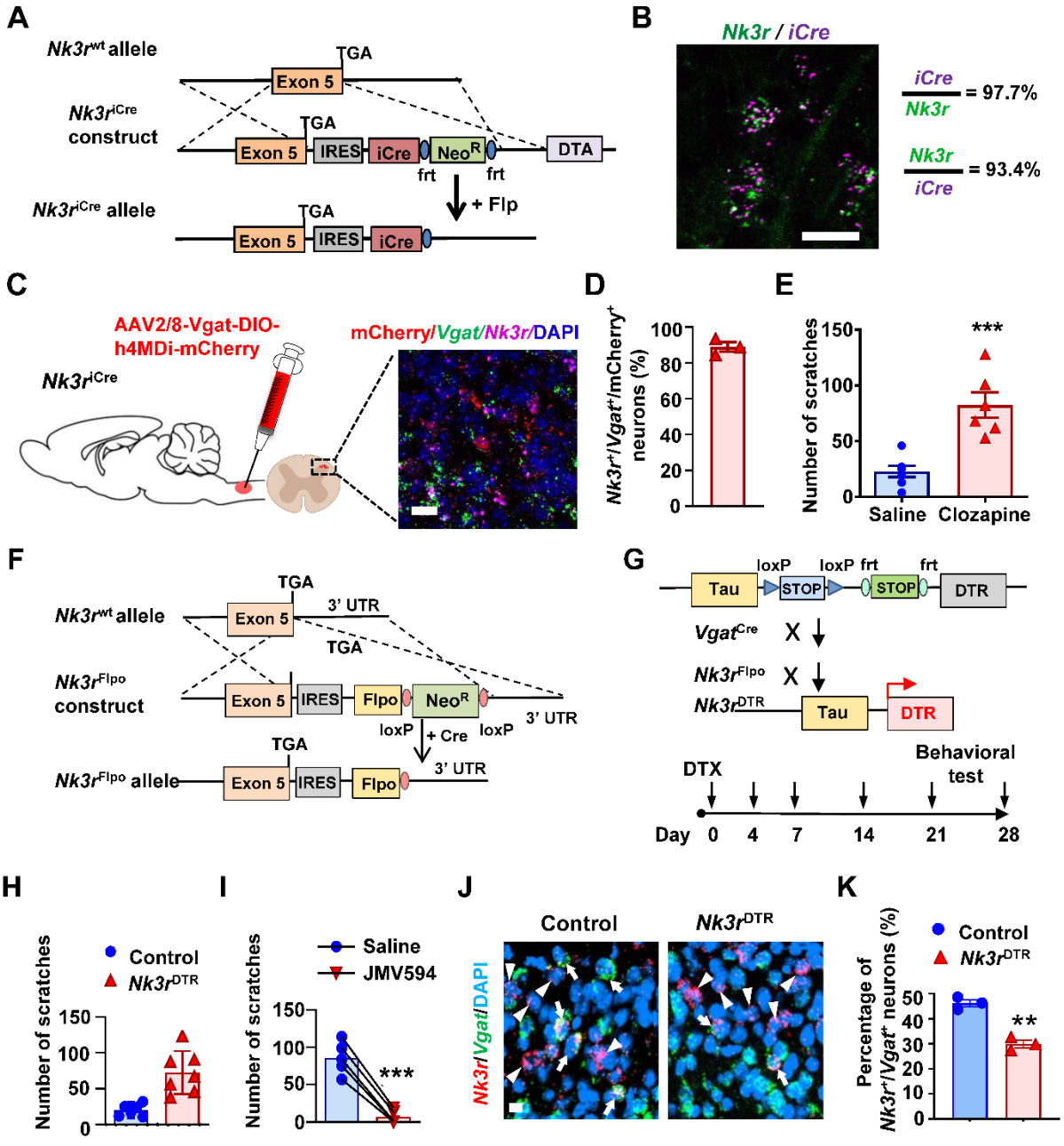

Figure 4. Selective inhibition and ablation of NK3R inhibitory neurons induce GRPR-dependent neuropathic itch.

(A) Generation of NK3R^{iCre} mice. **(B)** Double ISH confirming the co-expression of *Nk3r* and *iCre* in the superficial dorsal horn of the spinal cord. *iCre* mRNA was detected in 97.7% of *Nk3r*

neurons, and 93.4% of *Nk3r* neurons express *iCre*. Scale bar, 5 μm. $n = 4$ mice for each group. **(C)** Diagram showing the injection of AAV-Vgat-DIO-hM4Di-mCherry virus into the cervical spinal cord of $Nk3r^{iCre}$ mice. ISH image represents the co-expression of hM4Di-mCherry, *Vgat* and *Nk3r* in the superficial dorsal horn of $Nk3r^{iCre}$ mice. Scale bar, 20 μm. **(D)** Quantitative analysis demonstrating that over 85% of mCherry-positive neurons co-expressed *Nk3r* and *Vgat*. n = 3 mice. **(E)** Chemogenetic inactivation of *Nk3r* inhibitory neurons induced robust scratching behaviors. n = 6 mice per group. ***$p < 0.001$, unpaired *t*-test. **(F)** Generation of $NK3R^{Flpo}$ mice. **(G)** Intersectional genetic approach targeting ablation of *Nk3r* inhibitory neurons in the spinal cord. **(H)** Mice showed robust spontaneous scratching behaviors after ablation of *Nk3r* inhibitory neurons in the spinal cord. $n = 7$ mice per group. ***$p < 0.001$, unpaired *t*-test. **(I)** i.t. injection of GRPR antagonist JMV594 significantly blocked the neuropathic itch induced by chemogenetic inhibition of NK3R neurons. $n = 6$ mice. ***$p < 0.001$, paired *t*-test. **(J-K)** Representative ISH images of *Nk3r* and *Vgat* staining in dorsal horn of $Nk3r^{DTR}$ mice (J); the percentage of $Nk3r^{+}/Vgat^{+}$ neurons was significantly reduced in $Nk3r^{DTR}$ mice (K). Scale bar, 20 μm. $n = 3$ mice per group. **$p < 0.01$, unpaired *t*-test.

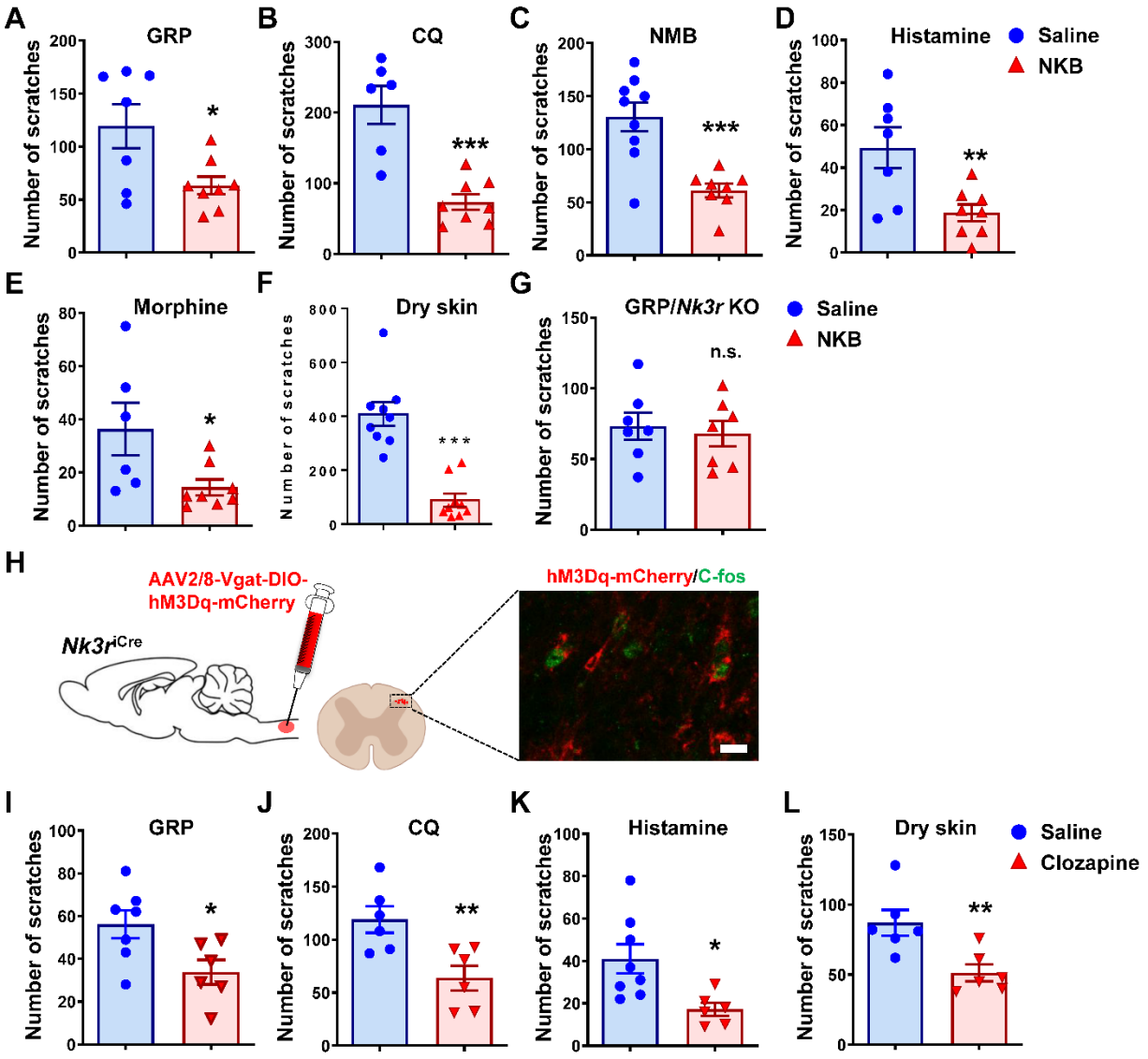

Figure 5. Activation of NK3R inhibitory neurons attenuates itch but not pain behaviors.

(A-E) i.t. injection of NKB (1 nmol) significantly inhibited scratching behaviors induced by GRP (0.3 nmol) (A), CQ (200 μg) (B), NMB (1 nmol) (C), histamine (200 μg) (D), and morphine (0.3 nmol) (E) in C57BL/6J mice. n = 6−10 mice per group. *$p < 0.05$, **$p < 0.01$, ***$p < 0.001$, unpaired t-test. **(F)** i.t. injection of NKB (1 nmol) significantly inhibited spontaneous scratching behaviors of dry skin mice. $n = 9$ mice per group. ***$p < 0.001$, unpaired t-test. **(G)** NKB (1 nmol)

did not affect GRP-induced scratching in *Nk3r* KO mice. n.s., not significant. **(H)** A diagram showing injection of Cre-dependent virus into the cervical spinal cord of *Nk3r*^{iCre} mice to express hM3Dq DREADD in the NK3R inhibitory neurons under the control of a *Vgat* promoter. Double IHC image showing clozapine-induced C-fos expression in *Nk3r*^{iCre} neurons infected by the hM3Dq-mCherry virus. Scale bar, 20 μm. **(I-L)** Chemogenetic activation of NK3R inhibitory neurons in the spinal cord by i.p. injection of clozapine (1 mg/kg) attenuated the scratching behaviors induced by GRP (I), CQ (J), histamine (K), and dry skin (L). n = 6-8 mice per group. *$p < 0.05$, **$p < 0.01$, unpaired *t*-test.

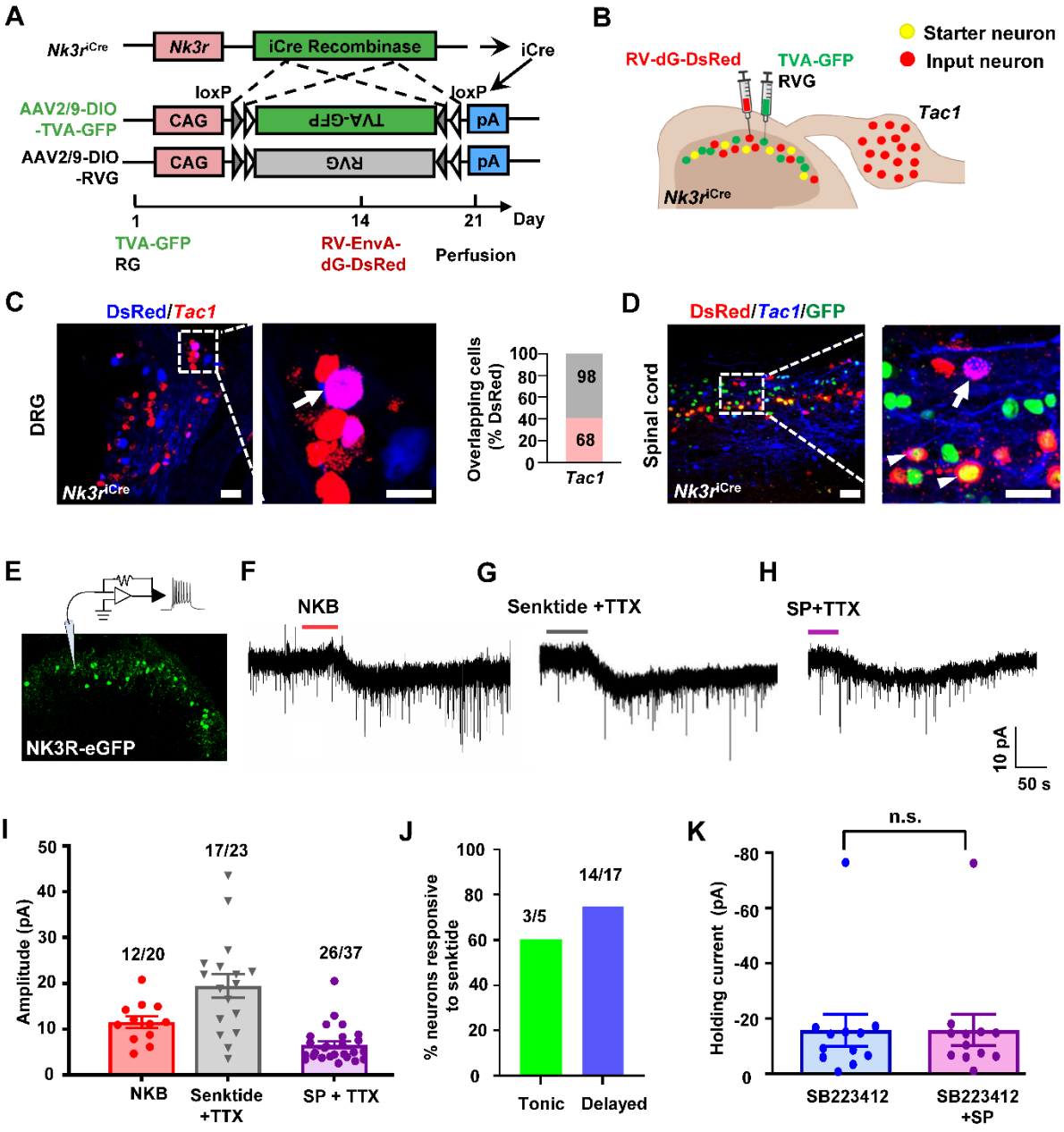

Figure 6. NK3R neurons form monosynaptic contacts with Tac1 sensory neurons and respond to neurokinins.

(A-B) Schematic diagram illustrating the experimental schedule (A) for monosynaptic tracing of input from *Tac1* sensory neurons and intraspinal injection of TVA-GFP/RG virus and RV-dG-DsRed virus (B). **(C)** Representative IHC images of *Tac1* staining in DRG neurons of *Nk3r*^{iCre}

mice (right: high power image of the boxed areas on the left). The graph shows that *Tac1* was expressed in 41% of DsRED neurons. $n = 3$ mice. Scale bar, 20 μm. **(D)** Representative ISH image of *Tac1*(blue) after RV*dG* injection (red). Arrowheads indicate *Nk3r*^{iCre} starter neurons (yellow) expressing GFP and DsRed. Arrows indicate *Tac1*$^{+}$ input neurons (DsRed^{+} and blue^{+}) targeting starter neurons. $n = 3$ mice. Scale bar, 100 μm. **(E)** A diagram showing the recording of NK3R-eGFP neurons in the superficial dorsal horn. **(F-H)** Representative slow inward currents evoked in NKR3 neurons by application of 1 μM NKB (F), 1 μM Senktide + 1 μM TTX (G), and 2 μM SP + 1 μM TTX (H), recorded in voltage clamp at -60 mV. **(I)** Peak amplitudes of the slow inward currents generated by the three agonists. Numbers above the bars indicate the responsive neurons. **(J)** Firing pattern characterization of neurons responding to senktide. Numbers above the bars indicate the responsive neurons. **(K)** Application of SP in the presence of the NK3R antagonist 3 μM SB223412 did not cause any significant change in the holding current (mean holding current amplitude in SB223412: -15.7 ± 5.7 pA; SB223412 + SP: -15.9 ± 5.7 pA; paired *t*-test, $p = 0.98$, $n = 12$).

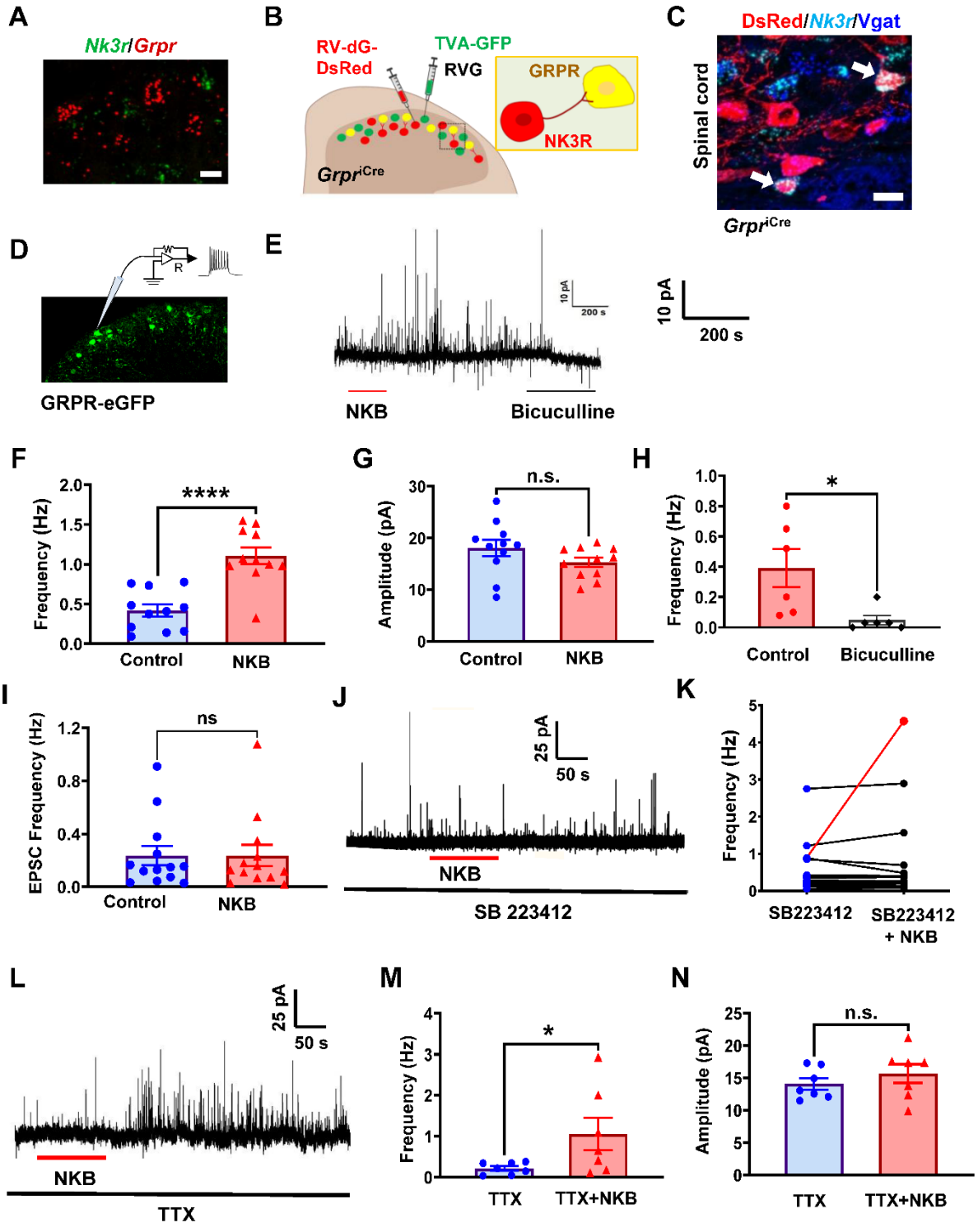

Figure 7. Activation of NK3R neurons by neurokinins inhibits GRPR neurons directly

(A) Representative double ISH images using RNAscope probes show that *Nk3r* neurons (green) do not co-express with *Grpr* (red). Scale bar, 20 μm. **(B)** Schematic of intraspinal injection of TVA-EGFP/RVG virus and RV-dG-dsRed virus on $Grpr^{iCre}$ mice. **(C)** Representative ISH image of *Nk3r* (teal) and *Vgat* (blue) in the cervical spinal cord after RV*dG* injections on $Grpr^{iCre}$ mice. The arrow indicates $Nk3r^{+}/Vgat^{+}$ input neurons targeting $Grpr^{iCre}$ neurons. $n = 3$ mice. Scale bar, 20 μm. **(D)** A diagram showing recording of GRPR-eGFP neurons in the superficial dorsal horn. **(E)** NKB (1 μM) induced a significant increase in the frequency of sIPSCs in a representative GRPR-eGFP neuron, recorded at -10 mV, while the frequency of sEPSCs (visible as inward currents) was not altered. The sIPSCs were almost completely blocked by bicuculline (20 μM), indicating the involvement of GABA release. **(F)** Changes of sIPSC frequency produced by NKB in a subpopulation of responsive GRPR-eGFP neurons (control: 0.4 ± 0.1 Hz, NKB: 1.1 ± 0.1 Hz, paired *t*-test, ****$p < 0.0001$, $n = 11/31$). **(G)** sIPSC amplitudes were not significantly affected by NKB application (control: 18.0 ± 1.6 pA; NKB: 15.3 ± 0.9 pA; paired *t*-test, $p = 0.12$, $n = 11$). **(H)** Change of sIPSC frequency after bicuculline application (20 μM), observed in a sample of GRPR neurons responsive to NKB, showing that sIPSCs are predominantly mediated by $GABA_A$ receptors (control = 0.4 ± 0.1 Hz; bicuculline: 0.04 ± 0.03 Hz, paired *t*-test, *$p < 0.05$, $n = 6$). **(I)** The frequency of glutamatergic sEPSCs was not significantly changed in a subset of GRPR neurons tested with NKB (control: 0.23 ± 0.07 Hz; NKB: 0.23 ± 0.08 Hz; paired *t*-test, $p = 0.98$, $n = 13$). **(J-K)** Representative trace of sIPSCs recorded from a GRPR-eGFP neuron in the presence of NKB and the NK3R antagonist SB223412 (3 μM, J). The effect of NKB on sIPSC frequency was blocked by the antagonist: only 1 out of 17 GRPR neurons responded (K, red symbol). **(L-N)** NKB caused a significant increase of mIPSC frequency in a subset of GRPR neurons in the presence of TTX (M: control: 0.2 ± 0.05 Hz; NKB: 1.1 ± 0.4 Hz; Wilcoxon Signed Rank test, *p

< 0.05; n = 7/21), while mIPSC amplitudes were not altered (N: control: 14.1 ± 0.9 pA; NKB: 15.7 ± 1.4 pA; paired t-test, p = 0.22; n = 7), confirming the presence of direct connections between inhibitory NK3R and GRPR neurons.

REFERENCES:

1. Chen, Z.F. (2021). A neuropeptide code for itch. Nature reviews. Neuroscience *22*, 758-776. https://doi.org/10.1038/s41583-021-00526-9.
2. Sun, Y.G., and Chen, Z.F. (2007). A gastrin-releasing peptide receptor mediates the itch sensation in the spinal cord. Nature *448*, 700-703. https://doi.org/10.1038/nature06029.
3. Sun, Y.G., Zhao, Z.Q., Meng, X.L., Yin, J., Liu, X.Y., and Chen, Z.F. (2009). Cellular basis of itch sensation. Science (New York, N.Y.) *325*, 1531-1534. https://doi.org/10.1126/science.1174868.
4. Mu, D., Deng, J., Liu, K.F., Wu, Z.Y., Shi, Y.F., Guo, W.M., Mao, Q.Q., Liu, X.J., Li, H., and Sun, Y.G. (2017). A central neural circuit for itch sensation. Science (New York, N.Y.) *357*, 695-699. http://doi.org/10.1126/science.aaf4918.
5. Chen, S., Gao, X.F., Zhou, Y., Liu, B.L., Liu, X.Y., Zhang, Y., Barry, D.M., Liu, K., Jiao, Y., Bardoni, R., et al. (2020). A spinal neural circuitry for converting touch to itch sensation. Nature communications *11*, 5074. https://doi.org/10.1038/s41467-020-18895-7.
6. Meng, Q.T., Liu, X.Y., Liu, X.T., Liu, J., Munanairi, A., Barry, D.M., Liu, B., Jin, H., Sun, Y., Yang, Q., et al. (2021). BNP facilitates NMB-encoded histaminergic itch via NPRC-NMBR crosstalk. eLife *10*. http://doi.org/10.7554/eLife.71689.
7. Wan, L., Jin, H., Liu, X.Y., Jeffry, J., Barry, D.M., Shen, K.F., Peng, J.H., Liu, X.T., Jin, J.H., Sun, Y., et al. (2017). Distinct roles of NMB and GRP in itch transmission. Scientific reports *7*, 15466. http://doi.org/10.1038/s41598-017-15756-0.
8. Prajapati, J.N., Shah, D.P., and Barik, A. (2025). An intra-brainstem circuitry for pain-induced inhibition of itch. Neuroscience *568*, 95-107. http://doi.org/10.1016/j.neuroscience.2025.01.008.
9. Zhao, Z.Q., Liu, X.Y., Jeffry, J., Karunarathne, W.K., Li, J.L., Munanairi, A., Zhou, X.Y., Li, H., Sun, Y.G., Wan, L., et al. (2014). Descending control of itch transmission by the serotonergic system via 5-HT1A-facilitated GRP-GRPR signaling. Neuron *84*, 821-834. 10.1016/j.neuron.2014.10.003.
10. Ikoma, A., Steinhoff, M., Stander, S., Yosipovitch, G., and Schmelz, M. (2006). The neurobiology of itch. Nature reviews. Neuroscience *7*, 535-547. https://doi.org/10.1038/nrn1950.
11. Davidson, S., Zhang, X., Khasabov, S.G., Simone, D.A., and Giesler, G.J., Jr. (2009). Relief of itch by scratching: state-dependent inhibition of primate spinothalamic tract neurons. Nature neuroscience *12*, 544-546. https://doi.org/10.1038/nn.2292.
12. Akiyama, T., Tominaga, M., Carstens, M.I., and Carstens, E.E. (2012). Site-dependent and state-dependent inhibition of pruritogen-responsive spinal neurons by scratching. The European journal of neuroscience *36*, 2311-2316. https://doi.org/10.1111/j.1460-9568.2012.08136.x.
13. Liu, M.Z., Chen, X.J., Liang, T.Y., Li, Q., Wang, M., Zhang, X.Y., Li, Y.Z., Sun, Q., and Sun, Y.G. (2019). Synaptic control of spinal GRPR(+) neurons by local and long-range inhibitory inputs. Proceedings of the National Academy of Sciences of the United States of America. https://doi.org/10.1073/pnas.1905658116.
14. Kardon, A.P., Polgar, E., Hachisuka, J., Snyder, L.M., Cameron, D., Savage, S., Cai, X., Karnup, S., Fan, C.R., Hemenway, G.M., et al. (2014). Dynorphin acts as a neuromodulator to inhibit itch in the dorsal horn of the spinal cord. Neuron *82*, 573-586. https://doi.org/10.1016/j.neuron.2014.02.046.
15. Boyle, K.A., Polgar, E., Gutierrez-Mecinas, M., Dickie, A.C., Cooper, A.H., Bell, A.M., Jumolea, E., Casas-Benito, A., Watanabe, M., Hughes, D.I., et al. (2023). Neuropeptide Y-expressing dorsal horn inhibitory interneurons gate spinal pain and itch signalling. eLife *12*. https://doi.org/10.7554/eLife.86633.

16. Zeng, Q., Li, Y., Wu, Y., Wu, J., Xu, K., Chen, Y., Rao, Y., Li, N., Luo, Y., Jiang, C., et al. (2025). Neuropeptide Y neurons mediate opioid-induced itch by disinhibiting GRP-GRPR microcircuits in the spinal cord. Nature communications *16*, 7074. http://dor.org/10.1038/s41467-025-62382-w.
17. Bourane, S., Duan, B., Koch, S.C., Dalet, A., Britz, O., Garcia-Campmany, L., Kim, E., Cheng, L., Ghosh, A., Ma, Q., and Goulding, M. (2015). Gate control of mechanical itch by a subpopulation of spinal cord interneurons. Science (New York, N.Y.) *350*, 550-554. https://doi.org/10.1126/science.aac8653.
18. Dai, D., Li, Z., Zhao, T., Li, Z., Tang, Y., Li, X., Gao, X.F., and Xiong, L. (2025). Downregulation of the NPY-Y1R system in Grpr neurons results in mechanical and chemical hyperknesis in chronic itch. Neurobiology of disease *206*, 106806. http://doi.org/10.1016/j.nbd.2025.106806.
19. Duan, B., Cheng, L., Bourane, S., Britz, O., Padilla, C., Garcia-Campmany, L., Krashes, M., Knowlton, W., Velasquez, T., Ren, X., et al. (2014). Identification of spinal circuits transmitting and gating mechanical pain. Cell *159*, 1417-1432. https://doi.org/10.1016/j.cell.2014.11.003.
20. Nelson, T.S., and Taylor, B.K. (2020). Targeting spinal neuropeptide Y1 receptor-expressing interneurons to alleviate chronic pain and itch. Prog Neurobiol, 101894. https://doi.org/10.1016/j.pneurobio.2020.101894.
21. Liu, H.X., and Hokfelt, T. (2002). The participation of galanin in pain processing at the spinal level. Trends Pharmacol Sci *23*, 468-474. http://doi.org/10.1016/s0165-6147(02)02074-6.
22. Fatt, M.P., Zhang, M.D., Kupari, J., Altinkok, M., Yang, Y., Hu, Y., Svenningsson, P., and Ernfors, P. (2024). Morphine-responsive neurons that regulate mechanical antinociception. Science (New York, N.Y.) *385*, eado6593. http://doi.org/10.1126/science.ado6593.
23. Geppetti, P., Veldhuis, N.A., Lieu, T., and Bunnett, N.W. (2015). G Protein-Coupled Receptors: Dynamic Machines for Signaling Pain and Itch. Neuron *88*, 635-649. http://doi.org/10.1016/j.neuron.2015.11.001.
24. Liu, B., Qiao, L., Liu, K., Liu, J., Piccinni-Ash, T.J., and Chen, Z.F. (2022). Molecular and neural basis of pleasant touch sensation. Science (New York, N.Y.) *376*, 483-491. http://dor.org/10.1126/science.abn2479.
25. Jordt, S.E., Bautista, D.M., Chuang, H.H., McKemy, D.D., Zygmunt, P.M., Hogestatt, E.D., Meng, I.D., and Julius, D. (2004). Mustard oils and cannabinoids excite sensory nerve fibres through the TRP channel ANKTM1. Nature *427*, 260-265. http://doi.org/10.1038/nature02282.
26. Bardoni, R., Shen, K.F., Li, H., Jeffry, J., Barry, D.M., Comitato, A., Li, Y.Q., and Chen, Z.F. (2019). Pain Inhibits GRPR Neurons via GABAergic Signaling in the Spinal Cord. Scientific reports *9*, 15804. http://doi.org/10.1038/s41598-019-52316-0.
27. Zieglgansberger, W. (2018). Substance P and pain chronicity. Cell Tissue Res. https://doi.org/10.1007/s00441-018-2922-y.
28. Steinhoff, M.S., von Mentzer, B., Geppetti, P., Pothoulakis, C., and Bunnett, N.W. (2014). Tachykinins and their receptors: contributions to physiological control and the mechanisms of disease. Physiological reviews *94*, 265-301. http://doi.org/10.1152/physrev.00031.2013.
29. Otsuka, M., and Yoshioka, K. (1993). Neurotransmitter functions of mammalian tachykinins. Physiological reviews *73*, 229-308. https://doi.org/10.1152/physrev.1993.73.2.229.
30. Allen, B.J., Rogers, S.D., Ghilardi, J.R., Menning, P.M., Kuskowski, M.A., Basbaum, A.I., Simone, D.A., and Mantyh, P.W. (1997). Noxious cutaneous thermal stimuli induce a graded release of endogenous substance P in the spinal cord: imaging peptide action in vivo. The Journal of neuroscience : the official journal of the Society for Neuroscience *17*, 5921-5927. https://doi.org/10.1523/JNEUROSCI.17-15-05921.
31. Duggan, A.W., Morton, C.R., Zhao, Z.Q., and Hendry, I.A. (1987). Noxious heating of the skin releases immunoreactive substance P in the substantia gelatinosa of the cat: a study with

antibody microprobes. Brain research *403*, 345-349. https://doi.org/10.1016/0006-8993(87)90073-4.

32. Allen, B.J., Li, J., Menning, P.M., Rogers, S.D., Ghilardi, J., Mantyh, P.W., and Simone, D.A. (1999). Primary afferent fibers that contribute to increased substance P receptor internalization in the spinal cord after injury. Journal of neurophysiology *81*, 1379-1390. https://doi.org/10.1152/jn.1999.81.3.1379.
33. Honor, P., Menning, P.M., Rogers, S.D., Nichols, M.L., Basbaum, A.I., Besson, J.M., and Mantyh, P.W. (1999). Spinal substance P receptor expression and internalization in acute, short-term, and long-term inflammatory pain states. The Journal of neuroscience : the official journal of the Society for Neuroscience *19*, 7670-7678. https://doi.org/10.1523/JNEUROSCI.19-17-07670.1999.
34. Basbaum, A.I. (1999). Spinal mechanisms of acute and persistent pain. Reg Anesth Pain Med *24*, 59-67. https://doi.org/10.1016/s1098-7339(99)90167-0.
35. Sinha, G.P., Prasoon, P., Smith, B.N., and Taylor, B.K. (2021). Fast A-type currents shape a rapidly adapting form of delayed short latency firing of excitatory superficial dorsal horn neurons that express the neuropeptide Y Y1 receptor. The Journal of physiology *599*, 2723-2750. https://doi.org/10.1113/JP281033.
36. Yasaka, T., Tiong, S.Y.X., Hughes, D.I., Riddell, J.S., and Todd, A.J. (2010). Populations of inhibitory and excitatory interneurons in lamina II of the adult rat spinal dorsal horn revealed by a combined electrophysiological and anatomical approach. Pain *151*, 475-488. https://doi.org/10.1016/j.pain.2010.08.008.
37. Salio, C., Ferrini, F., Bighinati, A., Lacivita, E., Leopoldo, M., and Bardoni, R. (2025). Differential synaptic inhibition and serotonin 5-HT(7) receptor-mediated modulation in identified dorsal horn neurons. Neurochem Int, 106011. https://doi.org/10.1016/j.neuint.2025.106011.
38. Punnakkal, P., von Schoultz, C., Haenraets, K., Wildner, H., and Zeilhofer, H.U. (2014). Morphological, biophysical and synaptic properties of glutamatergic neurons of the mouse spinal dorsal horn. The Journal of physiology *592*, 759-776. https://doi.org/10.1113/jphysiol.2013.264937.
39. Browne, T.J., Gradwell, M.A., Iredale, J.A., Madden, J.F., Callister, R.J., Hughes, D.I., Dayas, C.V., and Graham, B.A. (2020). Transgenic Cross-Referencing of Inhibitory and Excitatory Interneuron Populations to Dissect Neuronal Heterogeneity in the Dorsal Horn. Frontiers in molecular neuroscience *13*, 32. http://doi.org/10.3389/fnmol.2020.00032.
40. Zhao, Z.Q., Wan, L., Liu, X.Y., Huo, F.Q., Li, H., Barry, D.M., Krieger, S., Kim, S., Liu, Z.C., Xu, J., et al. (2014). Cross-inhibition of NMBR and GRPR signaling maintains normal histaminergic itch transmission. The Journal of neuroscience : the official journal of the Society for Neuroscience *34*, 12402-12414. https://doi.org/10.1523/JNEUROSCI.1709-14.2014.
41. Liu, X.Y., Liu, Z.C., Sun, Y.G., Ross, M., Kim, S., Tsai, F.F., Li, Q.F., Jeffry, J., Kim, J.Y., Loh, H.H., and Chen, Z.F. (2011). Unidirectional cross-activation of GRPR by MOR1D uncouples itch and analgesia induced by opioids. Cell *147*, 447-458. https://doi.org/10.1016/j.cell.2011.08.043.
42. Akiyama, T., Carstens, M.I., and Carstens, E. (2010). Spontaneous itch in the absence of hyperalgesia in a mouse hindpaw dry skin model. Neuroscience letters *484*, 62-65. https://doi.org/10.1016/j.neulet.2010.08.020.
43. Escalante, A., and Klein, R. (2020). Spinal Inhibitory Ptf1a-Derived Neurons Prevent Self-Generated Itch. Cell reports *33*, 108422. https://doi.org/10.1016/j.celrep.2020.108422.
44. Lucas-Romero, J., Rivera-Arconada, I., and Lopez-Garcia, J.A. (2024). Noise or signal? Spontaneous activity of dorsal horn neurons: patterns and function in health and disease. Pflugers Arch *476*, 1171-1186. http://doi.org/10.1007/s00424-024-02971-8.

45. Iwagaki, N., Garzillo, F., Polgar, E., Riddell, J.S., and Todd, A.J. (2013). Neurochemical characterisation of lamina II inhibitory interneurons that express GFP in the PrP-GFP mouse. Molecular pain *9*, 56. http://doi.org/10.1186/1744-8069-9-56.
46. Ganley, R.P., Iwagaki, N., del Rio, P., Baseer, N., Dickie, A.C., Boyle, K.A., Polgár, E., Watanabe, M., Abraira, V.E., Zimmerman, A., et al. (2015). Inhibitory Interneurons That Express GFP in the PrP-GFP Mouse Spinal Cord Are Morphologically Heterogeneous, Innervated by Several Classes of Primary Afferent and Include Lamina I Projection Neurons among Their Postsynaptic Targets. The Journal of neuroscience : the official journal of the Society for Neuroscience *35*, 7626-7642. http://doi.org/10.1523/jneurosci.0406-15.2015.
47. Iwagaki, N., Ganley, R.P., Dickie, A.C., Polgár, E., Hughes, D.I., Del Rio, P., Revina, Y., Watanabe, M., Todd, A.J., and Riddell, J.S. (2016). A combined electrophysiological and morphological study of neuropeptide Y-expressing inhibitory interneurons in the spinal dorsal horn of the mouse. Pain *157*, 598-612. http://doi.org/10.1097/j.pain.0000000000000407.
48. Hokfelt, T., Pernow, B., and Wahren, J. (2001). Substance P: a pioneer amongst neuropeptides. J Intern Med *249*, 27-40. http://doi.org/10.1046/j.0954-6820.2000.00773.x.
49. Sakai, K., Sanders, K.M., Lin, S.H., Pavlenko, D., Funahashi, H., Lozada, T., Hao, S., Chen, C.C., and Akiyama, T. (2020). Low-Threshold Mechanosensitive VGLUT3-Lineage Sensory Neurons Mediate Spinal Inhibition of Itch by Touch. The Journal of neuroscience : the official journal of the Society for Neuroscience *40*, 7688-7701. http://doi.org/10.1523/JNEUROSCI.0091-20.2020.
50. Abraira, V.E., and Ginty, D.D. (2013). The sensory neurons of touch. Neuron *79*, 618-639. http://doi.org/10.1016/j.neuron.2013.07.051.
51. Braz, J., Solorzano, C., Wang, X., and Basbaum, A.I. (2014). Transmitting Pain and Itch Messages: A Contemporary View of the Spinal Cord Circuits that Generate Gate Control. Neuron *82*, 522-536. http://doi.org/10.1016/j.neuron.2014.01.018.
52. Akiyama, T., Tominaga, M., Takamori, K., Carstens, M.I., and Carstens, E. (2014). Roles of glutamate, substance P, and gastrin-releasing peptide as spinal neurotransmitters of histaminergic and nonhistaminergic itch. Pain *155*, 80-92. http://doi.org/10.1016/j.pain.2013.09.011.
53. Acton, D., Ren, X.Y., Di Costanzo, S., Dalet, A., Bourane, S., Bertocchi, I., Eva, C., and Goulding, M. (2019). Spinal Neuropeptide Y1 Receptor-Expressing Neurons Form an Essential Excitatory Pathway for Mechanical Itch. Cell reports *28*, 625-+. 10.1016/j.celrep.2019.06.033.
54. Munanairi, A., Liu, X.Y., Barry, D.M., Yang, Q., Yin, J.B., Jin, H., Li, H., Meng, Q.T., Peng, J.H., Wu, Z.Y., et al. (2018). Non-canonical Opioid Signaling Inhibits Itch Transmission in the Spinal Cord of Mice. Cell reports *23*, 866-877. https://doi.org/10.1016/j.celrep.2018.03.087.
55. Nelson, T.S., Fu, W., Donahue, R.R., Corder, G.F., Hokfelt, T., Wiley, R.G., and Taylor, B.K. (2019). Facilitation of neuropathic pain by the NPY Y1 receptor-expressing subpopulation of excitatory interneurons in the dorsal horn. Scientific reports *9*, 7248. https://doi.org/10.1038/s41598-019-43493-z.
56. Mar, L., Yang, F.C., and Ma, Q. (2012). Genetic marking and characterization of Tac2-expressing neurons in the central and peripheral nervous system. Molecular brain *5*, 3. https://doi.org/10.1186/1756-6606-5-3.
57. Barry, D.M., Liu, X.T., Liu, B., Liu, X.Y., Gao, F., Zeng, X., Liu, J., Yang, Q., Wilhelm, S., Yin, J., et al. (2020). Exploration of sensory and spinal neurons expressing gastrin-releasing peptide in itch and pain related behaviors. Nature communications *11*, 1397. http://doi.org/10.1038/s41467-020-15230-y.
58. Maggi, C.A. (1995). The mammalian tachykinin receptors. Gen Pharmacol *26*, 911-944. https://doi.org/10.1016/0306-3623(94)00292-u.

59. Guard, S., and Watson, S.P. (1991). Tachykinin Receptor Types - Classification and Membrane Signaling Mechanisms. Neurochem Int *18*, 149-165. https://doi.org/10.1016/0197-0186(91)90180-L.
60. Barry, D.M., Li, H., Liu, X.Y., Shen, K.F., Liu, X.T., Wu, Z.Y., Munanairi, A., Chen, X.J., Yin, J., Sun, Y.G., et al. (2016). Critical evaluation of the expression of gastrin-releasing peptide in dorsal root ganglia and spinal cord. Molecular pain *12*. https://doi.org/10.1177/1744806916643724.
61. Todd, A.J. (2002). Anatomy of primary afferents and projection neurones in the rat spinal dorsal horn with particular emphasis on substance P and the neurokinin 1 receptor. Experimental physiology *87*, 245-249. https://doi.org/10.1113/eph8702351.
62. Todd, A.J. (2010). Neuronal circuitry for pain processing in the dorsal horn. Nature reviews. Neuroscience *11*, 823-836. https://doi.org/nrn2947/10.1038/nrn2947.
63. Mantyh, P.W., Rogers, S.D., Honore, P., Allen, B.J., Ghilardi, J.R., Li, J., Daughters, R.S., Lappi, D.A., Wiley, R.G., and Simone, D.A. (1997). Inhibition of hyperalgesia by ablation of lamina I spinal neurons expressing the substance P receptor. Science (New York, N.Y.) *278*, 275-279. https://doi.org/10.1126/science.278.5336.275.
64. Steinhoff, M., Oaklander, A.L., Szabo, I.L., Stander, S., and Schmelz, M. (2019). Neuropathic itch. Pain *160 Suppl 1*, S11-S16. https://doi.org/10.1097/j.pain.0000000000001551.
65. Oaklander, A.L. (2011). Neuropathic itch. Semin Cutan Med Surg *30*, 87-92. http://doi.org/10.1016/j.sder.2011.04.006.
66. Zhao, Z.Q., Huo, F.Q., Jeffry, J., Hampton, L., Demehri, S., Kim, S., Liu, X.Y., Barry, D.M., Wan, L., Liu, Z.C., et al. (2013). Chronic itch development in sensory neurons requires BRAF signaling pathways. The Journal of clinical investigation *123*, 4769-4780. https://doi.org/10.1172/JCI70528.
67. Wang, F., Flanagan, J., Su, N., Wang, L.C., Bui, S., Nielson, A., Wu, X., Vo, H.T., Ma, X.J., and Luo, Y. (2012). RNAscope: a novel in situ RNA analysis platform for formalin-fixed, paraffin-embedded tissues. J Mol Diagn *14*, 22-29. https://doi.org/10.1016/j.jmoldx.2011.08.002.
68. Akiyama, T., Carstens, M.I., and Carstens, E. (2010). Enhanced scratching evoked by PAR-2 agonist and 5-HT but not histamine in a mouse model of chronic dry skin itch. Pain *151*, 378-383. https://doi.org/10.1016/j.pain.2010.07.024.
69. Miyamoto, T., Nojima, H., Shinkado, T., Nakahashi, T., and Kuraishi, Y. (2002). Itch-associated response induced by experimental dry skin in mice. Jpn J Pharmacol *88*, 285-292. https://doi.org/10.1254/jjp.88.285.
70. Decosterd, I., and Woolf, C.J. (2000). Spared nerve injury: an animal model of persistent peripheral neuropathic pain. Pain *87*, 149-158. https://doi.org/10.1016/S0304-3959(00)00276-1.
71. Betelli, C., MacDermott, A.B., and Bardoni, R. (2015). Transient, activity dependent inhibition of transmitter release from low threshold afferents mediated by GABAA receptors in spinal cord lamina III/IV. Molecular pain *11*, 64. https://doi.org/10.1186/s12990-015-0067-5.
72. Ono, K., Asami, R., Miyahara, N., Nakanishi, O., and Inenaga, K. (2011). Neuronal effects of neurokinin B on the rat subfornical organ. Neuroreport *22*, 374-378. http://dor.org/10.1097/WNR.0b013e3283469645.

STAR★METHODS

KEY RESOURCES TABLE: see separate file

EXPERIMENTAL MODELS AND STUDY PARTICIPANT DETAILS

Experiments were conducted using 8–12-week-old male C57BL/6J mice purchased from The Jackson Laboratory. NK3R-eGFP and GRPR-eGFP mice were purchased from GENSAT, VGAT-ChR2-eYFP mice were purchased from The Jackson Laboratory. *Grpr*^{iCre} mice were generated in our lab [5]. All mice were housed in clear plastic cages (≤5 mice per cage) in a controlled environment maintained at ~23 °C and 50 ± 10% humidity, with food and water available *ad libitum*. Animals were kept on a 12-h light/dark cycle (lights on at 7:00 AM). All experiments were conducted in accordance with the guidelines of the National Institutes of Health, the International Association for the Study of Pain, and were approved by the Animal Studies Committee at Washington University School of Medicine, the Internal Animal Care and Use Committee of the Army Medical University, and the Institutional Animal Care and Use Committee (IACUC) at Shenzhen Bay Laboratory.

For electrophysiology experiments, NK3R-eGFP, GRPR-eGFP mice or VGAT-ChR2-eYFP (P20-P30) of either sex were used. Most of the experiments on NK3R-eGFP animals and the recordings from VGAT-ChR2-eYFP mice were performed at the University of Modena and Reggio Emilia and were approved by the Italian Ministry of Health following the Guide for the Care and Use of Laboratory Animals and the EU and Italian regulations on animal welfare.

Generation of *Nk3r*^{iCre} and *Nk3r*^{Flpo} mice

A genomic fragment of approximately 8 kb encompassing exon 5 of the *Tacr3 (Nk3r)* gene was amplified by PCR from a BAC clone (RP-23, clone 465M13; Thermo Fisher Scientific) using a high-fidelity polymerase (CloneAmp HiFi PCR Mix, Clontech) and inserted into the pBluescript

KS vector. To generate *Nk3r*^{iCre}, an IRES-iCre cassette together with an frt-flanked PGK-neomycin resistance cassette was introduced into the 3′ untranslated region immediately following the endogenous stop codon (TGA) via In-Fusion® HD cloning (Clontech). For *Nk3r*^{Flpo}, an IRES-Flpo cassette and a loxP-flanked PGK-neomycin selection cassette were inserted into the same 3′ UTR region using an identical strategy. A diphtheria toxin A (DTA) cassette was added distal to the 3′ homology arm to enable negative selection. Targeting vectors were linearized with SacII and electroporated into AB1 embryonic stem cells. After selection with G418 (200 ng/μL), correctly targeted ES cell clones were identified by PCR analysis of both the 5′ and 3′ integration sites. Verified clones were injected into C57BL/6J blastocysts to produce chimeric animals. Germline transmission was confirmed by PCR genotyping, followed by backcrossing of founders onto the C57BL/6J genetic background.

METHOD DETAILS

RNAscope *in situ* hybridization (ISH) and immunohistochemistry (IHC)

Conventional *in situ* hybridization (ISH) was conducted as previously described [60] using a digoxigenin-labeled antisense cRNA probe (Roche) targeting *Tacr3* (nucleotides 713–1243 of *Tacr3* mRNA; NCBI accession NM_021382.6). Mice aged 8–12 weeks were anesthetized with ketamine (100 mg/kg) and xylazine (15 mg/kg) and transcardially perfused with DEPC-treated PBS (pH 7.4), followed by fixation with 4% paraformaldehyde (PFA). Spinal cords were harvested, post-fixed for 2–4 h, and cryoprotected overnight at 4 °C in PBS containing 20% sucrose. Tissue was embedded and sectioned transversely at 20 μm using a Leica cryostat, and sections were mounted onto Superfrost Plus slides.

After proteinase K digestion and prehybridization, sections were incubated overnight at 65 °C with the *Tacr3* probe (2 μg/mL). Unbound probe was removed by high-stringency SSC washes and RNase A treatment (0.1 μg/mL, 30 min). Sections were blocked for 3 h in 20% sheep serum containing 0.1% Tween-20, then incubated overnight at 4 °C with an alkaline phosphatase–conjugated anti-digoxigenin antibody (0.5 μg/mL; Roche). Colorimetric detection was achieved by incubation with NBT/BCIP substrate solution for 12–16 h at room temperature, and reactions were terminated by fixation in 0.5% PFA. For GFP immunodetection following ISH, sections were incubated with a rabbit anti-GFP antibody, followed by a biotin-SP–conjugated donkey anti-rabbit secondary antibody, and visualized using 3,3′-diaminobenzidine (DAB; MilliporeSigma, D8001). At least three animals per group were analyzed, with a minimum of three sections examined per animal. Bright-field images were acquired using a Nikon Eclipse Ti-U microscope equipped with a Nikon DS-Fi2 camera.

Double-label RNAscope ISH was performed using the RNAscope Multiplex Fluorescent Reagent Kit v2 (Advanced Cell Diagnostics) according to the manufacturer's protocol for fixed frozen tissue [67]. Spinal cords were dissected, post-fixed for 2–4 h, and cryoprotected overnight in 20% sucrose at 4 °C. Tissue was embedded in OCT, sectioned transversely at 20 μm using a Leica cryostat, and thaw-mounted onto Superfrost Plus slides. Sections were treated sequentially with hydrogen peroxide, target retrieval reagents (15 min at near-boiling temperature), and Protease III Plus reagent (15 min). Hybridization was performed using probes directed against *Tacr3* (Tacr3-C2; GenBank NM_021382.6; bases 247–1253; Cat. No. 481671-C2) and *iCre* (iCre-C3; GenBank AY056050.1; bases 2–1028; Cat. No. 423321-C3). Following amplification and fluorescent labeling, sections were imaged on a Nikon C2+ confocal microscope using a 20× objective. Positive mRNA signals were defined as three or more punctate fluorescent dots localized to the

nucleus and/or cytoplasm. For co-expression analyses involving *Tacr3/Vgat, Galanin, Npy, Pdyn, Vglut2, iCre,* or *Grpr,* puncta associated with individual DAPI-stained nuclei were evaluated. Images were collected across the entire Tacr3-expressing neuronal population within each section. Cell quantification was performed by an investigator blinded to experimental conditions.

For fluorescent immunohistochemistry (IHC), sections were incubated with primary antibodies overnight at 4 °C, followed by incubation with fluorophore-conjugated secondary antibodies. Primary antibodies included: rabbit anti-GFP (1:1000, Molecular Probes, A11122), chicken anti-GFP (1:500, Aves Labs, GFP-1020), rabbit anti-CGRP (1:3000, Millipore, AB15360), isolectin B4 (IB4; 1:200, Sigma-Aldrich), rabbit anti-PKCγ (1:1000, Santa Cruz, SC-211), rabbit anti-NK1R (1:2000, Millipore, AB5060), mouse anti-GABA (1:1000, Chemicon), and rabbit anti-Pax2 (1:300, Thermo Fisher Scientific, 71-6000). Secondary antibodies included Alexa Fluor 488–conjugated donkey anti-rabbit, anti-chicken, or anti–guinea pig antibodies (1:1000; Jackson ImmunoResearch), as well as Cy3- or Cy5-conjugated donkey secondary antibodies (1:1000; Jackson ImmunoResearch). Fluorescent images were acquired using a Nikon C2+ confocal microscope, and quantitative image analysis for neuronal counts was performed using ImageJ software (NIH; version 1.34e).

Acute itch behavior

Behavioral experiments were conducted during the day (8 AM to 3 PM). The injection site was shaved at least 3 days before the experiments. Prior to testing, each mouse was acclimated for 30 min in a plastic arena (10 × 11 × 15 cm) and for 10 min to the recording conditions. For intradermal injections, CQ (200 μg, Sigma) and histamine (200 μg, Sigma-Aldrich) were dissolved in 50 μl saline. For intrathecal lumbar injections, GRP (0.3 nmol, GenScript) and NMB (1 nmol, Bachem) were dissolved in 10 μl saline. NKB (1 nmol, Bachem) was intrathecally administered either prior

to CQ or histamine injections or co-injected with GRP or NMB. Immediately after injection, mice were placed in transparent rectangular observation boxes and videotaped from the side. Videos were analyzed by an observer blinded to treatment and genotype. A scratch was defined as a hind limb lift toward the nape or head followed by replacement of the limb on the floor, regardless of the number of scratching strokes performed during this movement[3]. Only scratches directed at the injection site were counted over a 30-min period.

Dry skin itch

The dry skin model was generated following previously established protocols [68,69]. Briefly, mice had their nape shaved at least 3 days prior to the experiments. The skin was treated twice daily for 5–7 days with a 1:1 mixture of acetone (Sigma-Aldrich) and diethyl ether (Sigma-Aldrich) applied for 15 seconds, immediately followed by 30 seconds of distilled water (AEW). Control littermates were treated with distilled water alone for 45 seconds on the same schedule. Spontaneous scratching was monitored for 60 minutes in the early morning on days 5–7

Pain behavior

Thermal sensitivity

Thermal sensitivity was assessed using the Hargreaves test, the hot plate test, the tail flick test, and the acetone test. In the Hargreaves test, the plantar surface of the paw was exposed to a radiant heat beam with 10-min intervals between trials. Paw withdrawal latency was measured five times per animal and averaged for analysis. For the hot plate test, mice were placed on a heated surface (48, 52, or 56 °C), and the latency to lick a hindpaw or jump was recorded. Cutoff times were set at 2 min for 48 °C, 1 min for 52 °C, and 30 s for 56 °C to prevent tissue damage. In the tail flick test, the distal end of the tail was exposed to radiant heat at 10-min intervals, and latency to flick

was measured five times per animal and averaged. Cold sensitivity was evaluated using the acetone test. A drop of acetone was gently applied to the lateral plantar surface of the paw with a blunted syringe needle without touching the skin. Responses were scored over 1 min using a previously established 0–5 scale: 0, no response; 1, quick withdrawal, flick, sniff, or paw stamp; 2, jumping or paw shaking; 3, multiple lifts or paw licking; 4, prolonged paw lifting, licking, shaking, or jumping; 5, paw guarding.

Mechanical sensitivity

Mechanical sensitivity was evaluated using calibrated von Frey filaments. The lateral plantar surface of each hindpaw was stimulated five times at 10-second intervals. The paw withdrawal threshold was defined as the smallest filament that elicited a reflexive flinch in at least 3 of the 5 trials.

Capsaicin test

The capsaicin test was conducted via intraplantar injection into the left hindpaw (Sigma-Aldrich, M2028; 0.2 μg per animal in 20 μl saline with 10% ethanol). Animals were video-recorded for 5 minutes, and the duration of licking and flinching behaviors was quantified.

Complete Freund's adjuvant (CFA) assay

Persistent inflammatory pain was induced by injecting 20 μl of freshly prepared CFA (50% in saline) into the plantar surface of the right hindpaw. Thermal and mechanical hypersensitivities were assessed using the Hargreaves and von Frey tests, respectively.

Spared nerve injury (SNI)

SNI was performed as previously described [70]. Briefly, mice were anesthetized with a ketamine (90 mg/kg) and xylazine (10 mg/kg) cocktail. The three terminal branches of the sciatic nerve were

exposed, and the common peroneal and tibial nerves were transected, leaving the sural nerve intact. Muscle and skin were sutured in two layers. Mechanical hypersensitivity was assessed using the von Frey test.

Intraspinal virus injection

Intraspinal AAV injections were performed as previously described [54]. *Nk3r*^{iCre} mice were anesthetized with ketamine (90 mg/kg) and xylazine (10 mg/kg) intraperitoneally and received buprenorphine (BupSR, 0.5 mg/kg) for analgesia. To enable manipulation of scratching behavior at the nape region, the cervical vertebrae (C2–C6) were exposed, and the vertebral column was secured in a stereotaxic frame with spinal adaptors, following previously established procedures[5]. Surrounding tissue was carefully removed to expose the spinal cord, and the dura was incised with a sharp needle. AAV2/8-Vgat-DIO-hM3Dq-mCherry (2.0×10^{13} vg/mL), AAV2/8-Vgat-DIO-hM4Di-mCherry (2.0×10^{13} vg/mL), or AAV5-Ef1a-DIO-eYFP (2×10^{13} vg/mL) was injected into the left side of the spinal cord at three sites between successive vertebrae (C3–C5) using a Hamilton Neuros-syringe with a 34-gauge beveled needle (20° angle, catalog number: 65458-02). The needle was inserted into the dorsal spinal cord at an angle of ~35° to a depth of ~250 μm, targeting the superficial dorsal horn. About 300 nL of virus was infused at a rate of 50 nL/min using a Stoelting Quintessential Injector (QSI, catalog number: 53311), and the needle remained in place for 5 min after injection before being slowly withdrawn. The incision was closed with nylon sutures, and the site was treated with triple antibiotic ointment and lidocaine. To prevent infection, animals received subcutaneous enrofloxacin (2.5 mg/kg in saline). Mice were allowed to recover on a warming pad and were returned to their home cages for 2 weeks to permit viral expression before clozapine N-oxide (CNO) administration.

Electrophysiology recording

Spinal cord slice preparation

NK3R-eGFP, GRPR-eGFP or VGAT-ChR2-eYFP mice were anesthetized with isoflurane and decapitated. The spinal cord along with the vertebrae was rapidly removed and placed in ice-cold dissecting Krebs' solution (in mM: 95 NaCl, 50 sucrose, 2.5 KCl, 1.25 NaH_2PO_4, 26 $NaHCO_3$, 25 glucose, 6 $MgCl_2$, 1.5 $CaCl_2$, 1 kynurenic acid; pH 7.4; 320 mOsm) bubbled with 95% O_2 and 5% CO_2. The lumbar spinal cord was isolated, embedded in 3% low-melting-point agarose (Thermo Fisher Scientific), and transverse slices (400 μm) were prepared using a vibrating microtome (WPI). Slices were then maintained in oxygenated Krebs' solution (in mM: 125 NaCl, 50 sucrose, 2.5 KCl, 1.25 NaH_2PO4, 26 $NaHCO_3$, 25 glucose, 6 $MgCl_2$, 1.5 $CaCl_2$; pH 7.4; 320 mOsm) at 35 °C for 30 min before being used for recordings.

Patch clamp recording, dorsal root and optogenetic stimulation

Whole-cell patch-clamp recordings were performed at room temperature on visually identified NK3R-eGFP or GRPR-eGFP neurons. Neurons were visualized using a BX51WI microscope (Olympus) equipped with Nomarski optics and a CCD camera (Dage-MTI). Slices were perfused at 2 mL/min with recording Krebs' solution (in mM: 125 NaCl, 2.5 KCl, 1.25 NaH_2PO_4, 26 $NaHCO_3$, 25 glucose, 1 $MgCl_2$, 2 $CaCl_2$; pH 7.4; 320 mOsm). Recording pipettes (3–5 MΩ, thick-walled borosilicate) were filled with intracellular solution containing (in mM): 120 K-methanesulfonate, 10 NaCl, 10 EGTA, 1 $CaCl_2$, 10 HEPES, 5 ATP-Mg; pH 7.2 (adjusted with KOH), 300 mOsm. Inhibitory postsynaptic currents (IPSCs) in GRPR-eGFP neurons were recorded in voltage clamp at -10 mV using a cesium-based internal solution (in mM: 130 $CsMeSO_3$,

10 NaCl, 10 EGTA, 1 $CaCl_2$, 10 HEPES, 2 ATP-Mg; pH 7.3 with CsOH, 280–290 mOsm). Junction potentials were corrected post-recording. Signals were acquired with a Multiclamp 700A amplifier and pClamp 10 software (Molecular Devices), sampled at 10 kHz, and filtered at 2–5 kHz. To evoke excitatory postsynaptic currents (EPSCs), the dorsal root attached to each slice was stimulated using a suction electrode (0.1 ms pulse duration). Stimulus intensities were <25 μA for Aβ fibers, 25–100 μA for Aδ fibers, and 100–500 μA for C fibers. Monosynaptic versus polysynaptic EPSCs were determined by high-frequency stimulation. Following previous criteria [71], EPSCs showing no failures and constant latency (≤0.5 ms variability) during 20 consecutive stimulations at 20 Hz were classified as Aβ monosynaptic, at 10 Hz or 2 Hz as Aδ monosynaptic, and EPSCs showing no failures at 1 Hz (with variable latency) were classified as C monosynaptic. Channelrhodopsin-2 (ChR2)–mediated currents in VGAT-positive neurons from VGAT-ChR2-eYFP mice were evoked by a 500-ms pulse of blue light (470 nm; High-Power LED Collimator LCS-0470-03-22, controlled by a BioLED Light Source Control Module, Mightex). Currents were recorded at a holding potential of -60 mV with a 20 s intertrial interval. In VGAT-negative neurons, identical light stimulation evoked only outward IPSCs.

Patch clamp data analysis

Resting membrane potential (RMP) was measured within the first 5 min of recording, and neurons with RMP more positive than –50 mV were excluded. Firing patterns were determined in current-clamp mode by applying incremental current steps of 20 pA from a holding potential of approximately –80 mV, which facilitates the identification of delayed firing patterns by removing inactivation of the potassium I_A current [35]. Rheobase was defined as the minimal current required to elicit an action potential (AP). AP threshold was identified at the inflection point of the rising

phase, and AP amplitude was calculated as the difference between threshold and the peak of the first spike elicited at rheobase. First AP latency was measured as the time from current step onset to the first AP, and AP number was the total spikes fired during the step. Both latency and spike number were assessed at rheobase plus 80 pA.

Electrophysiological properties of NK3R neurons were subjected to clustering analysis using Orange data mining software (v3.38). Datasets were imported, Euclidean distances calculated, and hierarchical clustering performed using Ward's minimum variance method. Dendrograms were generated to visualize cluster output [39].

Spontaneous excitatory or inhibitory postsynaptic currents (sEPSCs or sIPSCs) were analyzed offline with MiniAnalysis (Synaptosoft). Changes in frequency or amplitude were assessed by Kolmogorov-Smirnov tests on cumulative distributions of inter-event intervals or current amplitudes. Exogenous compounds—including Senktide (1 μM), Capsaicin (1 μM), Menthol (500 μM), Substance P (2 μM), Bicuculline methobromide (20 μM), Strychnine hydrochloride (500 nM), TTX (1 μM), and SB 223412 (3 μM)—were bath-applied. All drugs were obtained from Sigma-Aldrich. The concentrations of the compounds used were consistent with those reported in previous electrophysiological studies on brain and spinal cord slices[72], also taking into account the limited drug penetration in this preparation.

Data were analyzed offline using pClamp 10 (Molecular Devices) or MiniAnalysis 6.0 (Synaptosoft), and graphs were prepared with SigmaPlot 16 (GraphPad).

Monosynaptic retrograde tracing

Briefly, 400 nL of a 1:1 mixture of rAAV2/9-Ef1α-DIO-EGFP-TVA and rAAV2/9-Ef1α-DIO-RVG (2.0×10^{12} vg/mL, BrainVTA) was injected into the cervical spinal cord of *Nk3r*^{iCre} or

Grpr^{iCre} mice. Two weeks later, 200 nL of RV-ENVA-dG-dsRed (2.0×10^8 IFU/mL, BrainVTA) was delivered at the same site. One week after rabies virus injection, mice were perfused, and the spinal cord and dorsal root ganglia (DRGs) were sectioned and imaged using a Nikon C2+ confocal microscope (Nikon Instruments). Sections were subsequently processed for RNAscope *in situ* hybridization with *Tac1*, *Nk3r*, and *Vgat* probes (Advanced Cell Diagnostics) and imaged under the confocal microscope. Pre- and post-ISH images were aligned and merged for analysis.

QUANTIFICATION AND STATISTICAL ANALYSIS

Statistical methods are indicated in the Fig. legends where used. Data are presented as mean ± standard error of the mean (SEM), statistical details of the experiments can be found in the figure legends. Analyses were performed using Prism 7 (v7.0d, GraphPad). For electrophysiological data, parametric comparisons between two groups were performed using a paired t-test, while non-parametric tests were applied when data were not normally distributed. For behavioral experiments, an F test was first used to assess variance equality between two groups, followed by Student's t-test to evaluate significance. For multiple comparisons, Bartlett's test was used to assess variance homogeneity, and two-way ANOVA followed by appropriate post hoc tests was applied to determine statistical significance. Significance levels are indicated as $*p < 0.05$, $**p < 0.01$, $***p < 0.001$, and $****p < 0.0001$. A p-value < 0.05 was considered statistically significant.

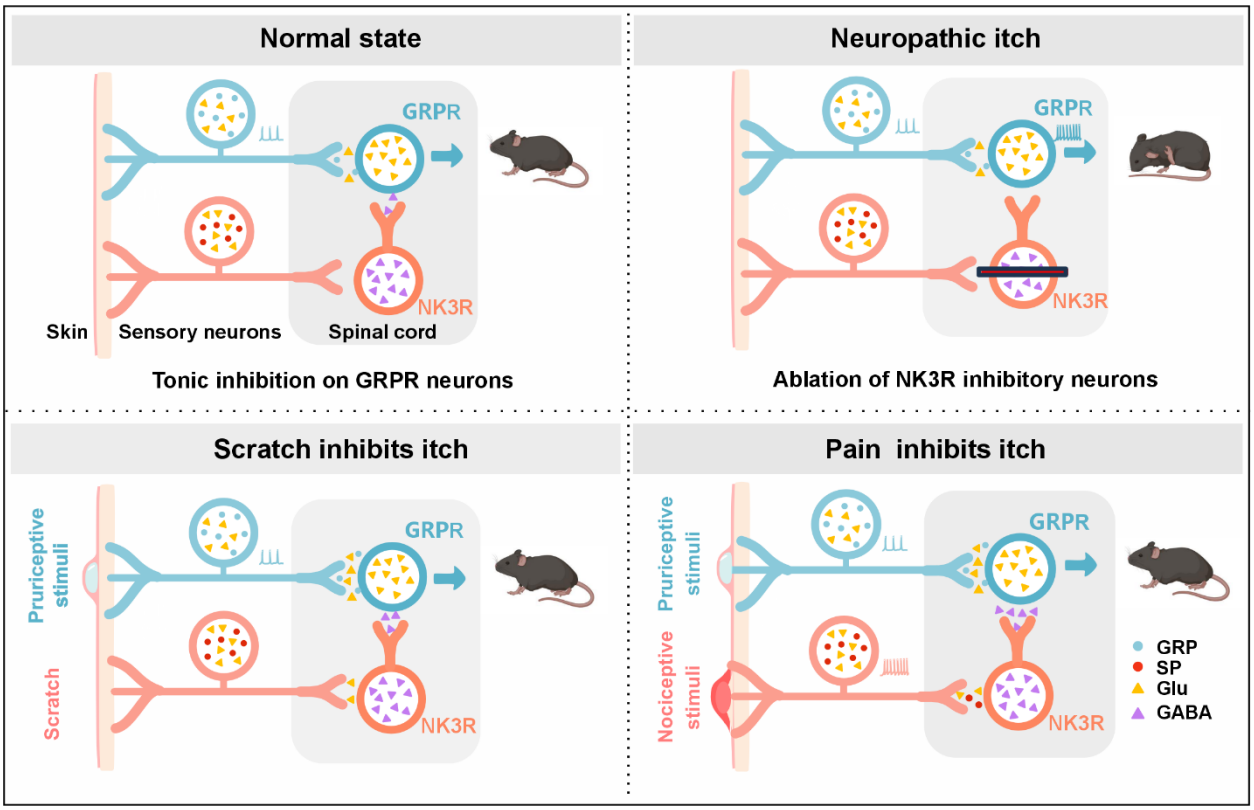

Highlights

NK3R inhibitory neurons exhibit distinct functional properties

NK3R inhibitory neurons tonically gate itch, not pain

NK3R neurons form monosynaptic contacts with *Tac1* afferents and GRPR neurons

Substance P activates NK3R interneurons in the dorsal horn

eTOC blurb

Shen et al. identify a population of dorsal horn inhibitory neurons that express neurokinin 3 (NK3R) receptors. They receive monosynaptic input from nociceptive primary afferents—including those releasing substance P—and project directly to itch-processing GRPR neurons. Silencing this inhibitory NK3R population disinhibits GRPR neurons, thereby triggering neuropathic itch.

CELL PRESS DECLARATION OF INTERESTS POLICY

Transparency is essential for a reader's trust in the scientific process and for the credibility of published articles. At Cell Press, we feel that disclosure of competing interests is a critical aspect of transparency. Therefore, we require a "declaration of interests" section in which all authors disclose any financial or other interests related to the submitted work that (1) could affect or have the perception of affecting the author's objectivity or (2) could influence or have the perception of influencing the content of the article.

What types of articles does this apply to?

We require that you disclose competing interests for all submitted content by completing and submitting the form below. We also require that you include a "declaration of interests" section in the text of all articles even if there are no interests to declare.

What should I disclose?

We require that you and all authors disclose any personal financial interests (e.g., stocks or shares in companies with interests related to the submitted work or consulting fees from companies that could have interests related to the work), professional affiliations, advisory positions, board memberships (including membership on a journal's advisory board when publishing in that journal), or patent applications and/or registrations that are related to the subject matter of the contribution. As a guideline, you need to declare an interest for (1) any affiliation associated with a payment or financial benefit exceeding $10,000 p.a. or 5% ownership of a company or (2) research funding by a company with related interests. You do not need to disclose diversified mutual funds, 401ks, or investment trusts.

Authors should also disclose relevant financial interests of immediate family members. Cell Press uses the Public Health Service definition of "immediate family member," which includes spouse and dependent children.

Where do I declare competing interests?

Competing interests should be disclosed on this form as well as in a "declaration of interests" section in the manuscript. This section should include financial or other competing interests as well as affiliations that are not included in the author list. Examples of "declaration of interests" language include:

> "AUTHOR is an employee and shareholder of COMPANY."
> "AUTHOR is a founder of COMPANY and a member of its scientific advisory board."

NOTE: Primary affiliations should be included with the author list and do not need to be included in the "declaration of interests" section. Funding sources should be included in the "acknowledgments" section and also do not need to be included in the "declaration of interests" section. (A small number of front-matter article types do not include an "acknowledgments" section. For these articles, reporting of funding sources is not required.)

What if there are no competing interests to declare?

If you have no competing interests to declare, please note that in the "declaration of interests" section with the following wording:

> "The authors declare no competing interests."

CELL PRESS DECLARATION OF INTERESTS FORM

If submitting materials via Editorial Manager, please complete this form and upload with your initial submission. Otherwise, please email as an attachment to the editor handling your manuscript.

Please complete each section of the form and insert any necessary "declaration of interests" statement in the text box at the end of the form. A matching statement should be included in a "declaration of interests" section in the manuscript.

Institutional affiliations

We require that you list the current institutional affiliations of all authors, including academic, corporate, and industrial, on the title page of the manuscript. ***Please select one of the following:***

☒ All affiliations are listed on the title page of the manuscript.

☐ I or other authors have additional affiliations that we have noted in the "declaration of interests" section of the manuscript and on this form below.

Funding sources

We require that you disclose all funding sources for the research described in this work. ***Please confirm the following:***

☒ All funding sources for this study are listed in the "acknowledgments" section of the manuscript.*

*A small number of front-matter article types do not include an "acknowledgments" section. For these, reporting funding sources is not required.

Competing financial interests

We require that authors disclose any financial interests and any such interests of immediate family members, including financial holdings, professional affiliations, advisory positions, board memberships, receipt of consulting fees, etc., that:

(1) could affect or have the perception of affecting the author's objectivity, *or*
(2) could influence or have the perception of influencing the content of the article.

Please select one of the following:

☒ We, the authors and our immediate family members, have no financial interests to declare.

☐ We, the authors, have noted any financial interests in the "declaration of interests" section of the manuscript and on this form below, and we have noted interests of our immediate family members.

Advisory/management and consulting positions

We require that authors disclose any position, be it a member of a board or advisory committee or a paid consultant, that they have been involved with that is related to this study. We also require that members of our journal advisory boards disclose their position when publishing in that journal. ***Please select one of the following:***

☒ We, the authors and our immediate family members, have no positions to declare and are not members of the journal's advisory board.

☐ The authors and/or their immediate family members have management/advisory or consulting relationships noted in the "declaration of interests" section of the manuscript and on this form below.

Patents

We require that you disclose any patent applications and/or registrations related to this work by any of the authors or their institutions. ***Please select one of the following:***

☒ We, the authors and our immediate family members, have no related patent applications or registrations to declare.

☐ We, the authors, have a patent application and/or registration related to this work, which is noted in the "declaration of interests" section of the manuscript and on this form below, and we have noted the patents of immediate family members.

Please insert any "declaration of interests" statements in this space. This exact text should also be included in the "declaration of interests" section of the manuscript. If no authors have a competing interest, please insert the text, "The authors declare no competing interests."

The authors report no competing interests.

☒ **On behalf of all authors, I declare that I have disclosed all competing interests related to this work. If any exist, they have been included in the "declaration of interests" section of the manuscript.**